CrossMark

# The EURONEAR Lightcurve Survey of Near Earth Asteroids

O. Vaduvescu[1,2,3] · A. Aznar Macias[4] · V. Tudor[1] ·
M. Predatu[5] · A. Galád[6] · Š. Gajdoš[6] · J. Világi[6] ·
H. F. Stevance[1,7] · R. Errmann[1] · E. Unda-Sanzana[8] ·
F. Char[8] · N. Peixinho[8,9] · M. Popescu[10,11] · A. Sonka[10] ·
R. Cornea[12] · O. Suciu[12] · R. Toma[12,13] · P. Santos-Sanz[14] ·
A. Sota[14] · J. Licandro[2,3] · M. Serra-Ricart[2,3] ·
D. Morate[2,3] · T. Mocnik[1,15] · M. Diaz Alfaro[1,16] ·
F. Lopez-Martinez[1,17] · J. McCormac[1] · N. Humphries[1]

**Abstract** This data paper presents lightcurves of 101 near Earth asteroids (NEAs) observed mostly between 2014 and 2017 as part of the EURONEAR photometric survey using 11 telescopes with diameters between 0.4 and 4.2 m located in Spain, Chile, Slovakia and Romania. Most targets had no published data at the time of observing, but some objects were observed in the same period mainly by B. Warner, allowing us to confirm or improve the existing results. To plan the runs and select the targets, we developed the public *Long Planning* tool in PHP. For preliminary data reduction and rapid follow-up planning we developed the *LiDAS* pipeline in Python and IRAF. For final data reduction, flux calibration, night linkage and Fourier fitting, we used mainly *MPO Canopus*. Periods

---

✉ O. Vaduvescu
ovidiu.vaduvescu@gmail.com

[1]   Isaac Newton Group of Telescopes (ING), Apto. 321, 38700 Santa Cruz de la Palma, Canary Islands, Spain

[2]   Instituto de Astrofísica de Canarias (IAC), C/Vía Láctea, 38205 La Laguna, Tenerife, Spain

[3]   Departamento de Astrofísica, Universidad de La Laguna, 38206 La Laguna, Tenerife, Spain

[4]   Isaac Aznar Observatory, Aras de los Olmos, Valencia, Spain

[5]   Faculty of Sciences, University of Craiova, A. I. Cuza 13, 200585 Craiova, RO, Romania

[6]   Modra Observatory, Department of Astronomy, Physics of the Earth and Meteorology, FMPI UK, 84248 Bratislava, Slovakia

[7]   Department of Physics and Astronomy, University of Sheffield, Hounsfield Rd, Sheffield S3 7RH, UK

[8]   Unidad de Astronomía, Facultad Ciencias Básicas, Universidad de Antofagasta, Avda. Universidad de Antofagasta, 02800 Antofagasta, Chile

[9]   CITEUC - Centre for Earth and Space Science Research of the University of Coimbra, Observatório Geofísico e Astronómico da Universidade de Coimbra, 3030-004 Coimbra, Portugal

⌂ Springer

of 18 targets are presented for the first time, and we could solve or constrain rotation for 16 of them. We secured periods for 45 targets ($U \sim 3$), found candidate periods for other 16 targets ($U \sim 2$), and we propose tentative periods for other 32 targets ($U \sim 1$). We observed 7 known or candidate binary NEAs, fiting 3 of them (2102 Tantalus, 5143 Heracles and 68348). We observed 8 known or candidate tumbling NEAs, deriving primary periods for 3 objects (9400, 242708 and 470510). We evidenced rapid oscillations (few minutes) and could fit fast tentative periods $TP2$ for 5 large newly suggested tumbling or binary candidates (27346, 112985, 285625, 377732, 408980), probably discovering at least one new binary NEA (2011 WO41). We resolved periods of 4 special objects which include two proposed space mission targets (163249 and 101955 Bennu), one very fast rotator NEA discovered by EURONEAR (2014 NL52) and the "Halloween asteroid" (2015 TB145). Using Mercator in simultaneous 3 band MAIA imaging, we could evidence for the first time clear variation in the color lightcurves of 10 NEAs. The periods derived from the $g-r$ color lightcurves are found to match individual band period fits for 4 NEAs (27346, 86067, 112985 and 275976).

# 1 Introduction

In a cosmogonic context, the study of near Earth objects (NEOs) is essential to understand the origin and the evolution of our Solar System, the apparition of life on Earth and how the cosmic hazards could affect it. The improvement of the orbital and physical knowledge of near Earth asteroids (NEAs) is important for assessing the evolution of the small bodies in the context of gravitational perturbations by major planets and other subtle influences like the YORP/Yarkovsky and space weathering effects. The study of NEOs is vital due to their potential threat to Earth, evidenced by past impact events like super-bolides, known craters and mass extinctions. In this sense, growing the physical knowledge about NEOs is essential for planning space missions aiming to mitigate preventive actions against potential impacts. From the ground, photometry, spectroscopy, radar and stellar occultations are the most commonly used observing techniques aimed to derive the main physical properties of NEAs such as their size, shape, rotation, spin axis, taxonomy, albedo, binarity (multiplicity) and morphology.

[10]  Astronomical Institute of the Romanian Academy, 5 Cutitul de Argint, 040557 Bucharest, Romania

[11]  IMCCE, Observatoire de Paris, PSL Research University, CNRS, Sorbonne Universités, UPMC Univ Paris 06, Univ. Lille, Paris, France

[12]  Romanian Society for Meteors and Astronomy (SARM), CP 14 OP 1, 130170 Targoviste, Romania

[13]  Armagh Observatory and Planetarium, College Hill, Armagh BT61 9DG, Northern Ireland

[14]  Instituto de Astrofísica de Andalucía, IAA-CSIC, Apt 3004, 18080 Granada, Spain

[15]  Astrophysics Group, Keele University, ST5 5BG Staffordshire, UK

[16]  National Solar Observatory, 3010 Coronal Loop, 88349 Sunspot, NM, USA

[17]  Instituto de Astrofísica e Ciências do Espaço, Universidade do Porto, CAUP, Rua das Estrelas, Porto 4150-762, Portugal

Currently we know more than 16,000 NEAs discovered mostly by six U.S.-lead surveys (Spacewatch, LONEOS, NEAT, LINEAR, Catalina and Pan-STARRS). Nevertheless, only extremely few NEAs (about 7%) have been characterized photometrically via lightcurves. We briefly remind here the pioneering efforts of Pravec et al. (1995, 1996, 1997, 1998a, 2006); Galád et al. (2005) using 1 m class and smaller telescopes mostly during coordinated campaigns and those of T. Kwiatkowski et al. who used the giant SALT 10 m telescope to characterize very small objects presumably fast rotators (Kwiatkowski et al. 2005a; Kwiatkowski 2005b; Kwiatkowski et al. et al. 2005c). Small amateur telescopes (mostly 0.3–0.6 m diameter), as well as small professional telescopes (mostly 1-m class, some unsubscribed or dormant) could bring important contributions, especially those located in good weather sites. In this sense, we praise the efforts of the North-American amateurs Brian D. Warner and Robert D. Stephens who observed about 500 NEA lightcurves since 1999 from the actual number of around one thousand NEAs having valid lightcurves (uncertainty factor $U \geq 2-$), according to Warner (private communication) who counted recently the Lightcurve Asteroids Database (Warner 2009) (LCDB).[1]

Using genetic inversion techniques for sparse photometric data (Cellino et al. 2009), large field surveys of the ecliptic could bring substantial contributions to physical characterization of main belt asteroids (MBAs). One such survey was the *Thousand Asteroid Lightcurve Survey* (TALCS) conducted with CFHT in Sep 2006 which produced 278 rotation periods (Masiero et al. 2009). Another survey is the *Palomar Transient Factory* (Waszczak et al. 2015) which produced 88 quality periods plus 85 possible periods (Polishook et al. 2012). NEAs remain spread on the sky and they need targeted observing campaigns accessible for only few weeks around opposition, which require extended telescope effort difficult to secure via regular time applications for most professional facilities. In 2008 Brian Skiff et al. started the *Lowell Observatory NEA Photometric Survey* (NEAPS) aimed as a 3 year program using 4 telescopes from which finally only the LONEOS 0.55 m with 40′ and large scale 2.5″/pixel) was used. The NEAPS results were published in two Minor Planet Bulletins, adding 86 NEAs (Skiff et al. 2012; Koehn et al. 2009) observed in 2008 and 2009. Very recently, the *Mission Accessible Near-Earth Objects Survey* (MANOS) published photometric results consisting in rotational periods and amplitudes for 86 NEOs observed since 2013 using 1–4 m telescopes (Thirouin et al. 2016), targeting mostly newly discovered and smaller (sub-km) objects.

Since 2006 the *European Near Earth Asteroids Research* project (EURONEAR) has been improving the orbital and physical knowledge of NEAs part of an European network which includes 14 nodes from 7 European countries plus Chile.[2] In this context, in 2014 we started a NEA photometry survey using available telescopes in the EURONEAR network and by March 2017 we observed more than 150 objects. The first paper published 17 NEA lightcurves observed with two small telescopes (Aznar Macias, et. al. 2017). The actual data paper is the second in this series and publishes lightcurves and photometric data for 101 NEAs observed with 11 telescopes with diameters between 0.4 and 4.2 m. Two other papers will follow soon, the third presenting the 2015 Teide Observatory campaign (observed by R. Cornea, data reduction in work), while the fourth paper will characterize fast rotator NEAs using the LCOGT telescopes (lead by T. Kwiatkowski in 2015–2016). Many of our targets were selected to have literature spectra or/and were observed by EURO-NEAR using the Isaac Newton Telescope part of a spectroscopic survey to be published

---

[1] http://www.minorplanet.info/lightcurvedatabase.html.

[2] http://www.euronear.org.

soon (Popescu et. al. 2017), and we plan to join the photometric and spectroscopic data in a final science paper.

This paper is organised as follows: Sect. 2 presents the observing facilities. Section 3 addresses the planning tools, image reduction and lightcurve analysis software. Section 4 includes the observed objects and derived periods, grouping the targets in 7 sub-sections. The lightcurves and fitted periods are presented in Figs. 1, 2, 3, 4, 5, 6, 7, 8, 9 and 10 (ordered based on the telescope and asteroid number or designation), while the raw data and some tentative period fits of poorly observed objects are presented in the Appendix Figs. 12, 13, 14, 15, 16 and 17. Section 5 and Fig. 11 presents the color lightcurves and colors indices for the targets observed with the Mercator telescope. Finally, Sect. 6 draws the conclusions.

## 2 The Observing Facilities

Eleven telescopes with diameters between 0.4 and 4.2 m based in four countries (Spain, Chile, Slovakia and Romania) were accessed mostly between 2014 and 2017 (adding few older objects) by some EURONEAR members to observe lightcurves of 101 NEAs. We present first these observing facilities here, resuming their technical characteristics and total observed time (ObsT) in Table 1.
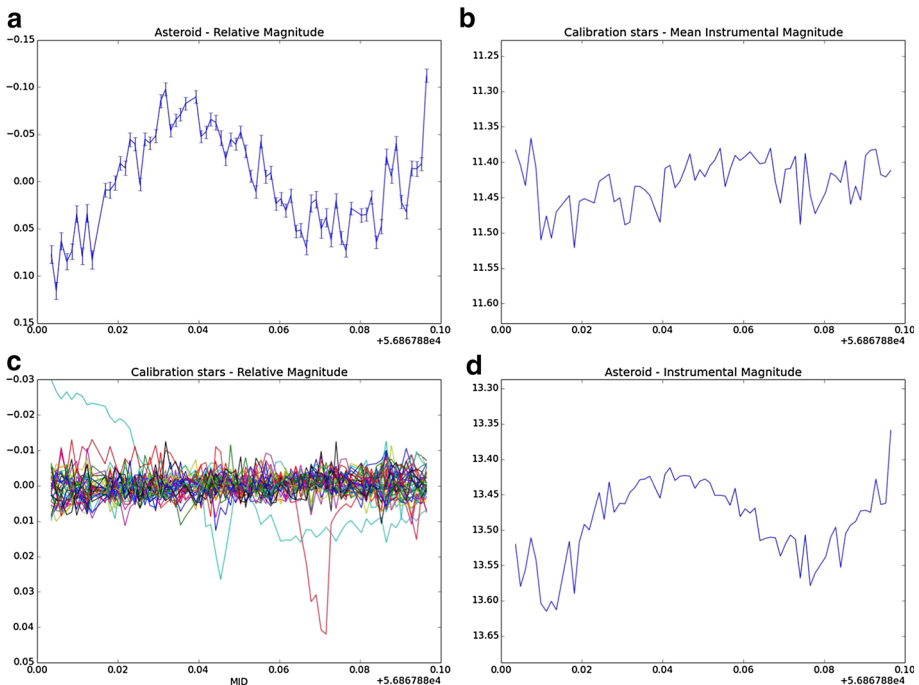


**Fig. 1** LiDAS sample output for the first night INT observations of the NEA (24443) on 29 July 2014. Two stars (in *green* and *red*) deviate by more than 2 sigma in a few measurements and they were automatically rejected from the final calibration
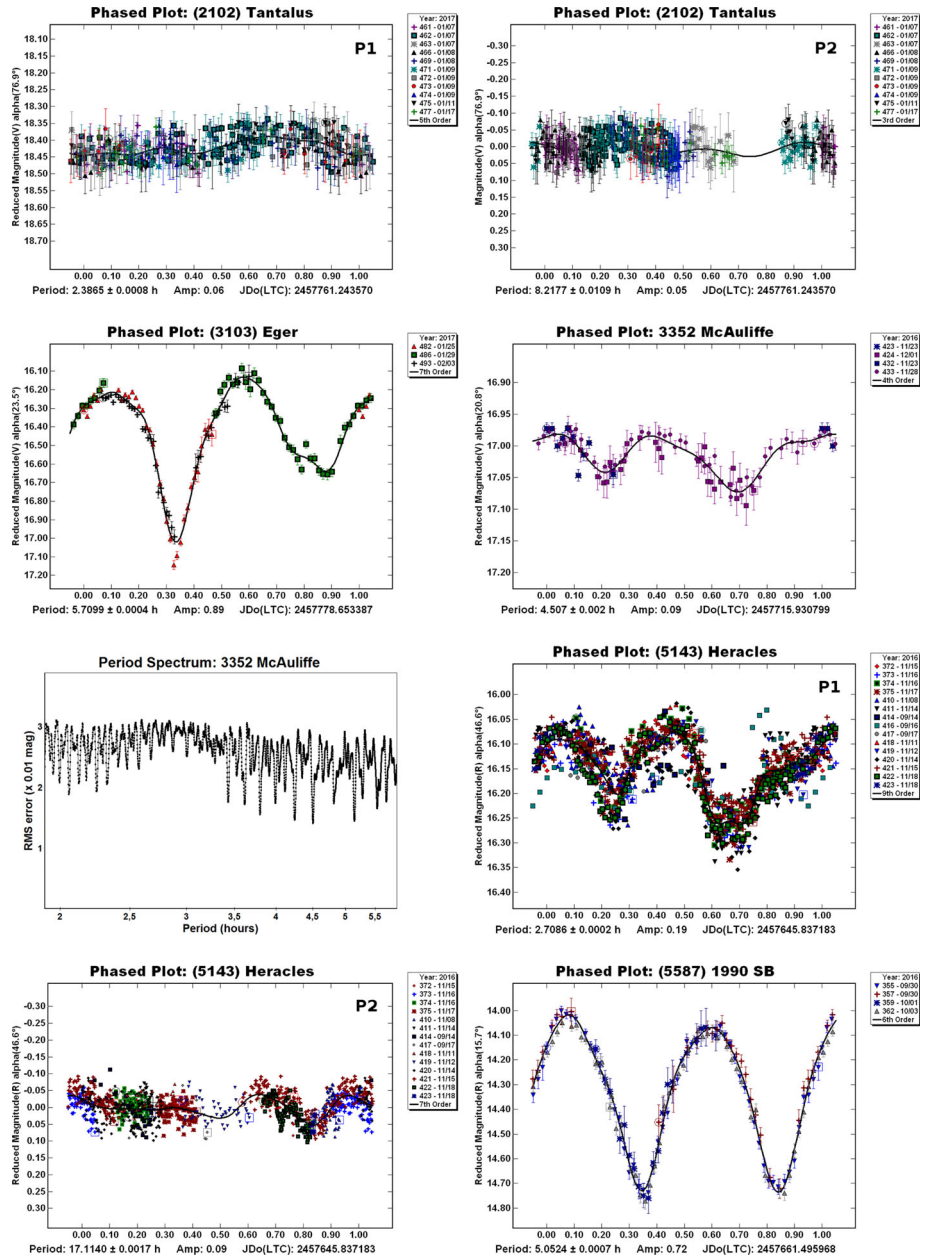
**Fig. 2** Lightcurves of NEAs observed with the IAO-T35 telescope (secured and candidate periods)

## 2.1 The Isaac Aznar 0.36 m Telescope in Spain (IAO-T35)

The *Isaac Aznar Observatory* (IAO) is privately owned by the Spanish amateur astronomer Amadeo Aznar in the province of Valencia. It is located in Aras de los Olmos, at 1270 m above the sea level, in one of the darkest night-sky of the Iberian Peninsula (limiting
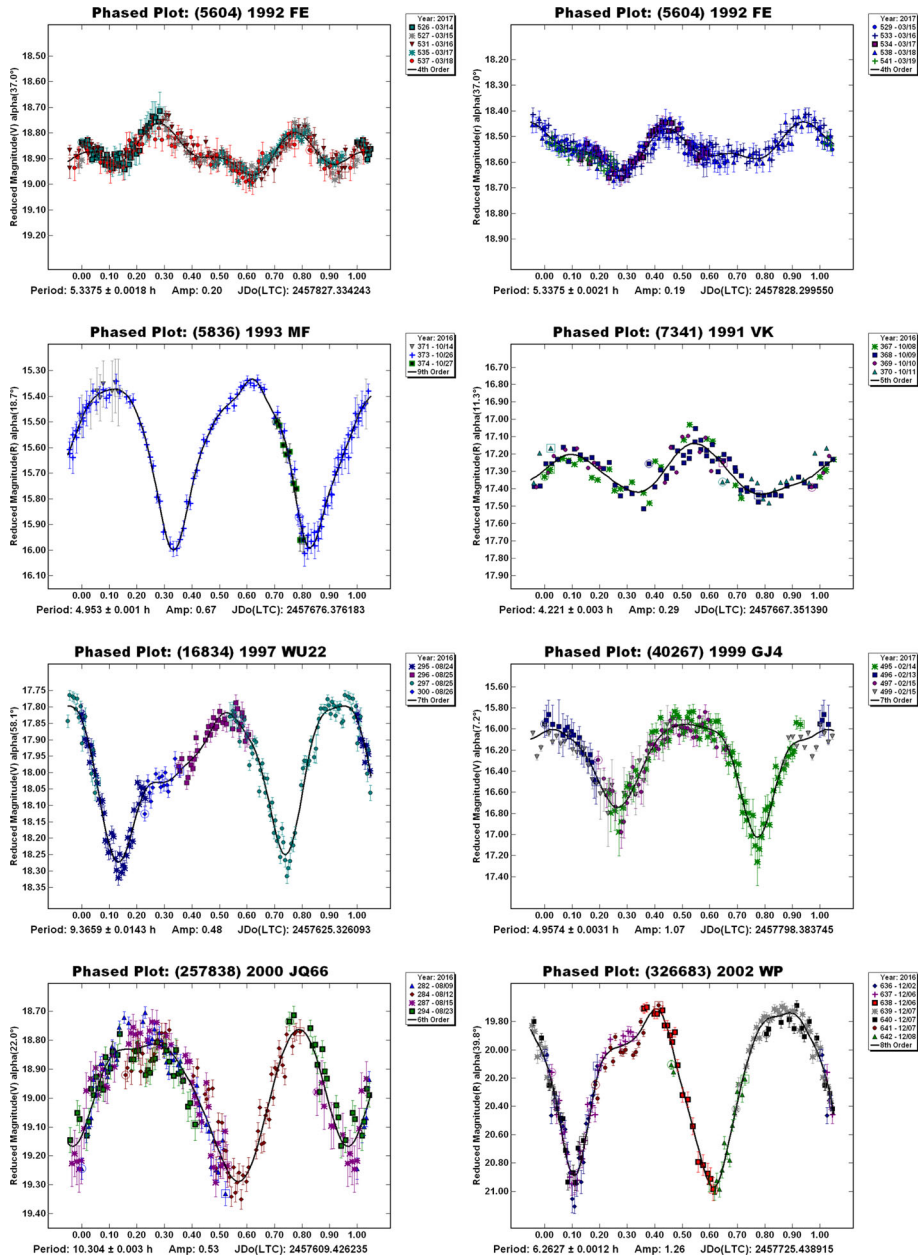
**Fig. 2** continued

magnitude 21.8 mag/arcsec$^2$). The optical system consists in a remotely controlled 0.36 m Schmidt-Cassegrain *F*/10 Meade LX200 telescope. The CCD camera is a SBIG STL 1001e with adaptive optics and CCD 1024 × 1024 pixels of size 24.6 μm, resulting in 1.44 ″/pixel and a square 25′ field. The camera holds broad band Astrodon Sloan *r* and Johnson *V* filters, working at −20 C with cooled water in the summer. Typical seeing at IAO is around 2 ″.
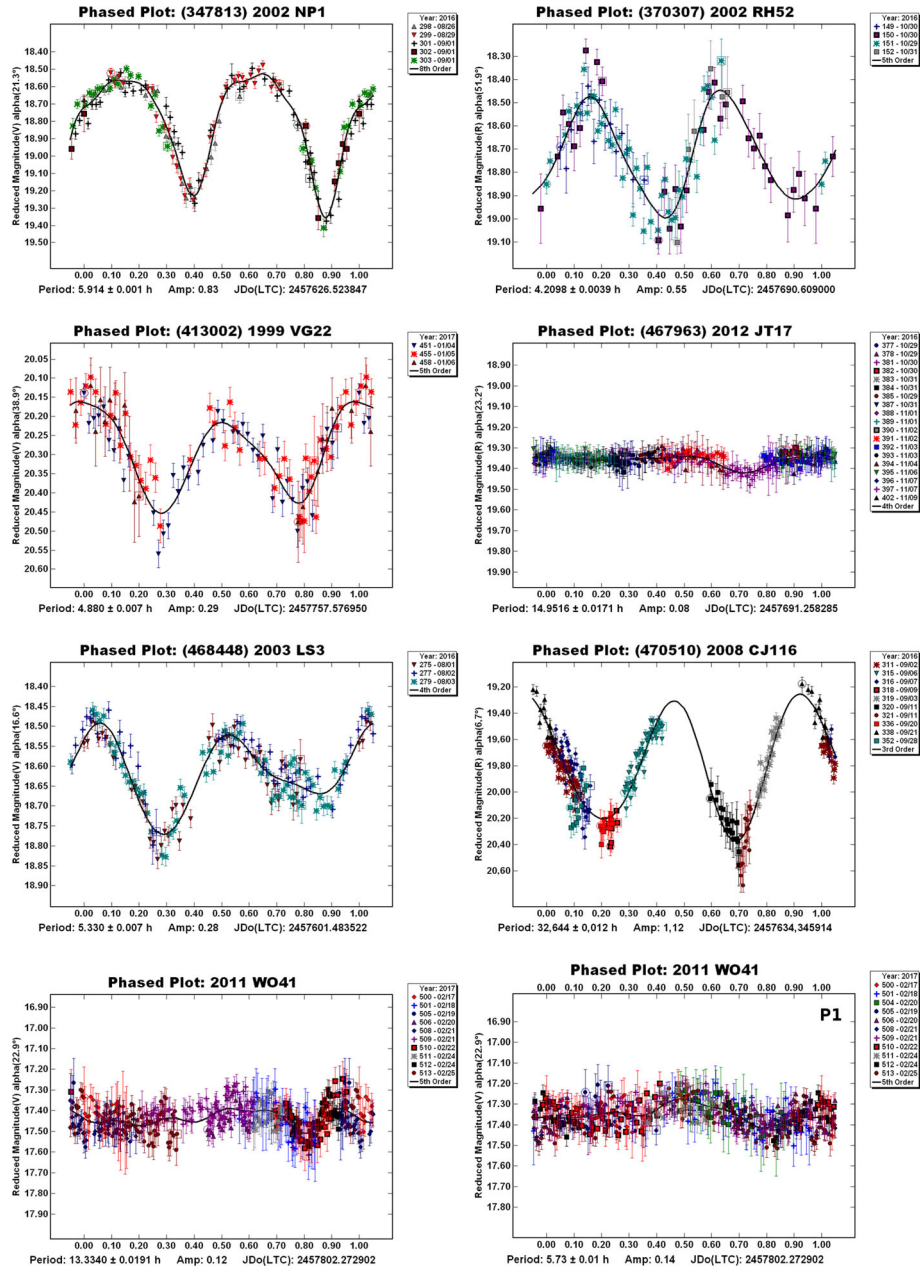
**Fig. 2** continued
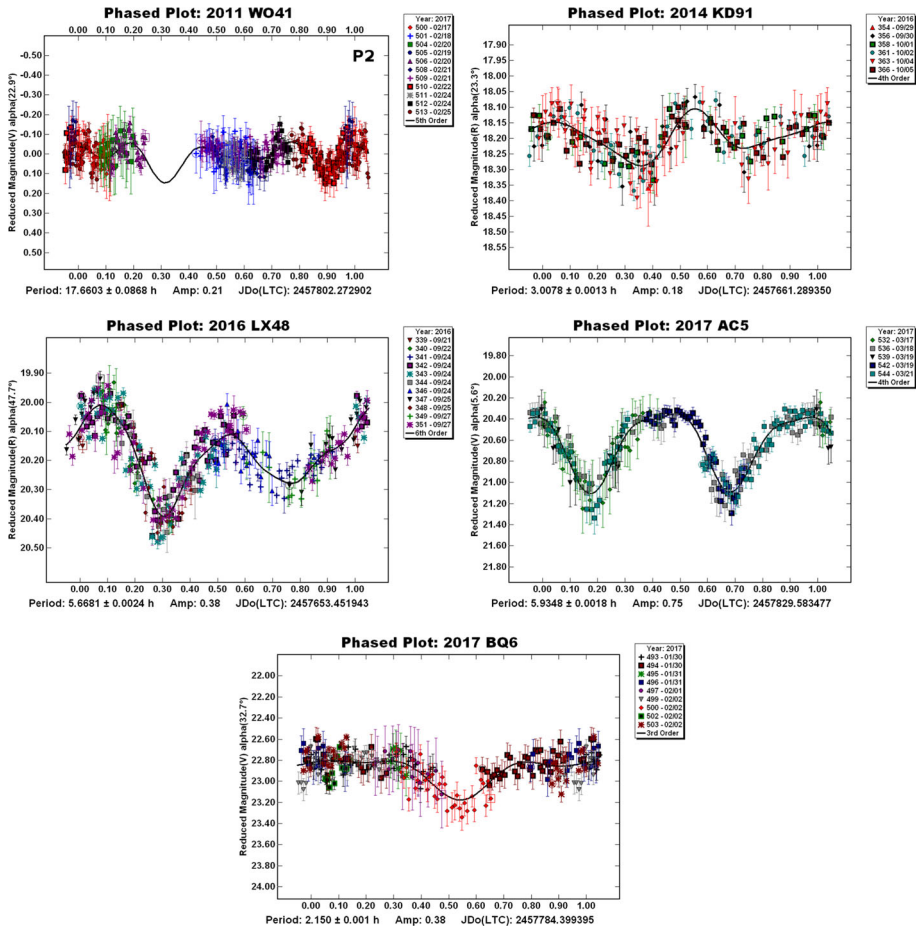
**Fig. 2** continued

## 2.2 The T50 0.5 m Telescope in Romania (Buc-T50)

This 0.5 m diameter *F*/10 Zeiss Cassegrain telescope is located at the historic Bucharest Observatory run by the Astronomical Institute of the Romanian Academy (AIRA). At its Cassegrain focus sits the SBIG camera STL-11000M with 4008 × 2745 9 μm pixels providing 16′ × 11′ rectangular field cooled at -20 C. The typical seeing in Bucharest is ∼3″ which allows binning 2 × 2 at a scale of 0.50″/pixel to be used. Broad band Johnson *UBVRI* filters are available, but no filter is used for lightcurve observations in order to increase the signal to noise.

## 2.3 The Caisey SON 0.5 m Telescope in Chile (SON-T50)

This *F*/8 0.51 m telescope is owned by the Finish private *Searchlight Observatory Network* (SON), being installed at the *SpaceObs* private observatory run in San Pedro de Atacama, Chile (2450 meters altitude). The camera brand is Apogee Alta U42 with 2048 × 2048
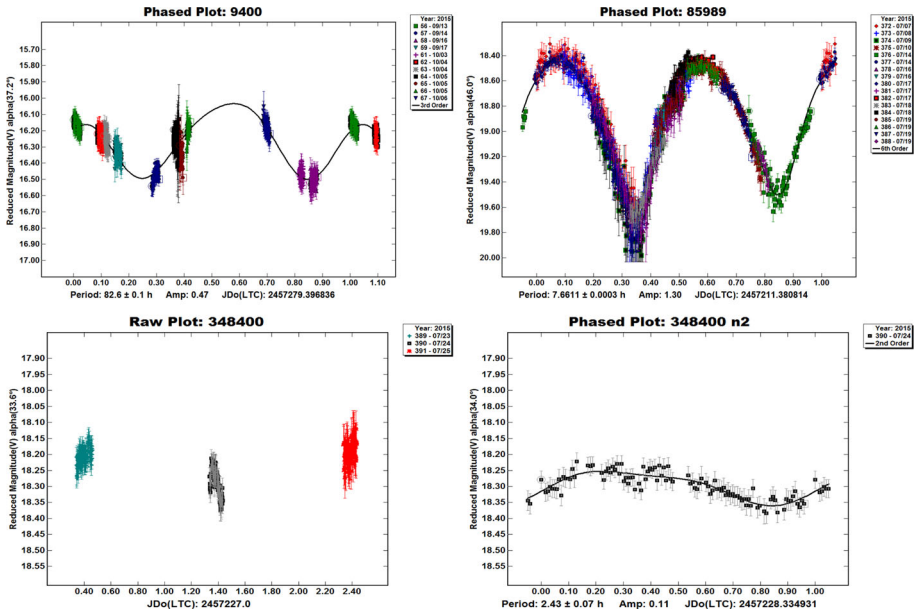
**Fig. 3** Lightcurves of NEAs observed with the Buc-T50 telescope (secured and candidate periods)

**Fig. 4** Lightcurve of NEA (214088) observed with the SON-T50 telescope (secured and candidate periods)
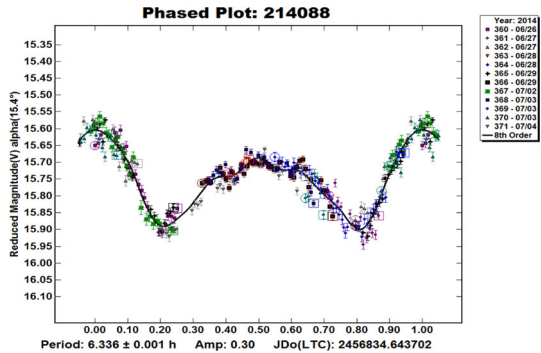


pixels of 13.5 μm which provide 0.80″/pixel and a 27.3′ square field. We observed one target in clear mode (no filter). Typical seeing in San Pedro de Atacama is around 1.5″.

## 2.4 The Modra 0.6 m Telescope in Slovakia (Mod-T60)

This 0.6 m diameter F/5.5 Zeiss telescope is located at the Astronomical and Geophysical Observatory (AGO) close to Modra, Slovakia, in the dark Southern region of Malé Karpaty mountains (530 m altitude), being owned and operated by the Comenius University, Bratislava. The camera brand is Apogee Ap8p, counting $1024 \times 1024$ pixels of 24 μm which provide 1.5″/pixel and a square 25′ field. The camera temperature is controlled for about 40 C bellow the ambient. We observed without filters under typical seeing around 3″.
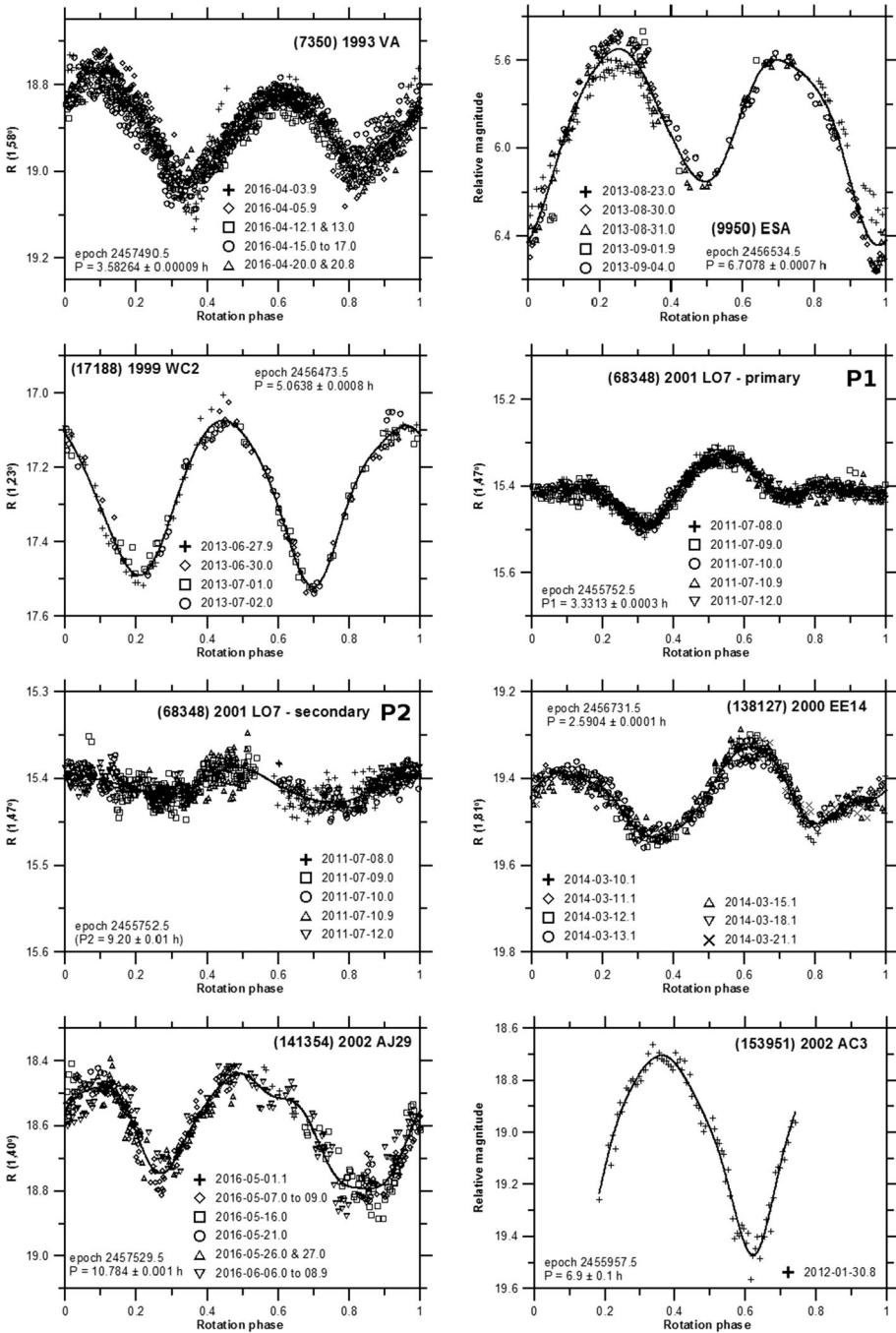
**Fig. 5** Lightcurves of NEAs observed with the MOD-T60 telescope (secured and candidate periods)
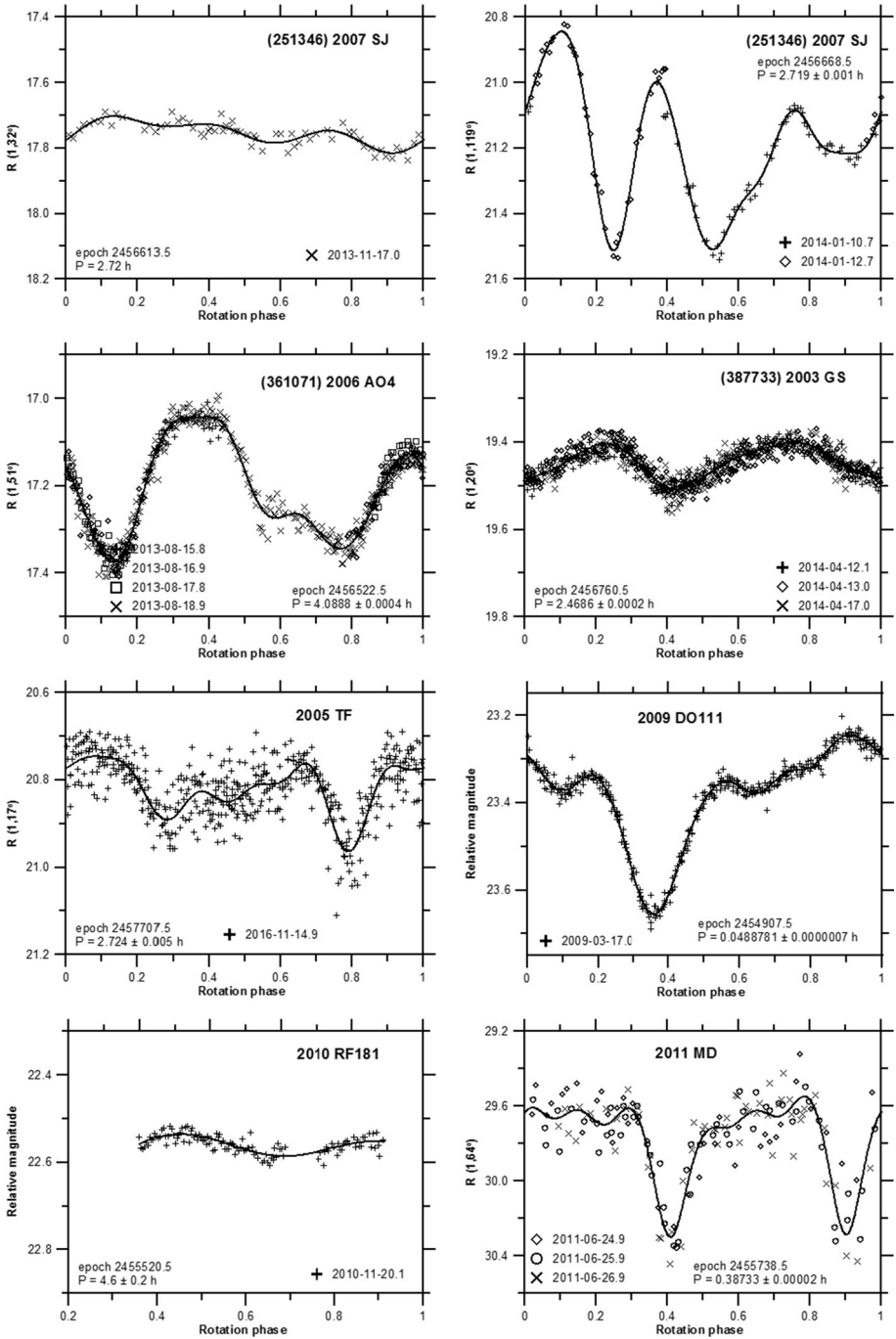
**Fig. 5** continued
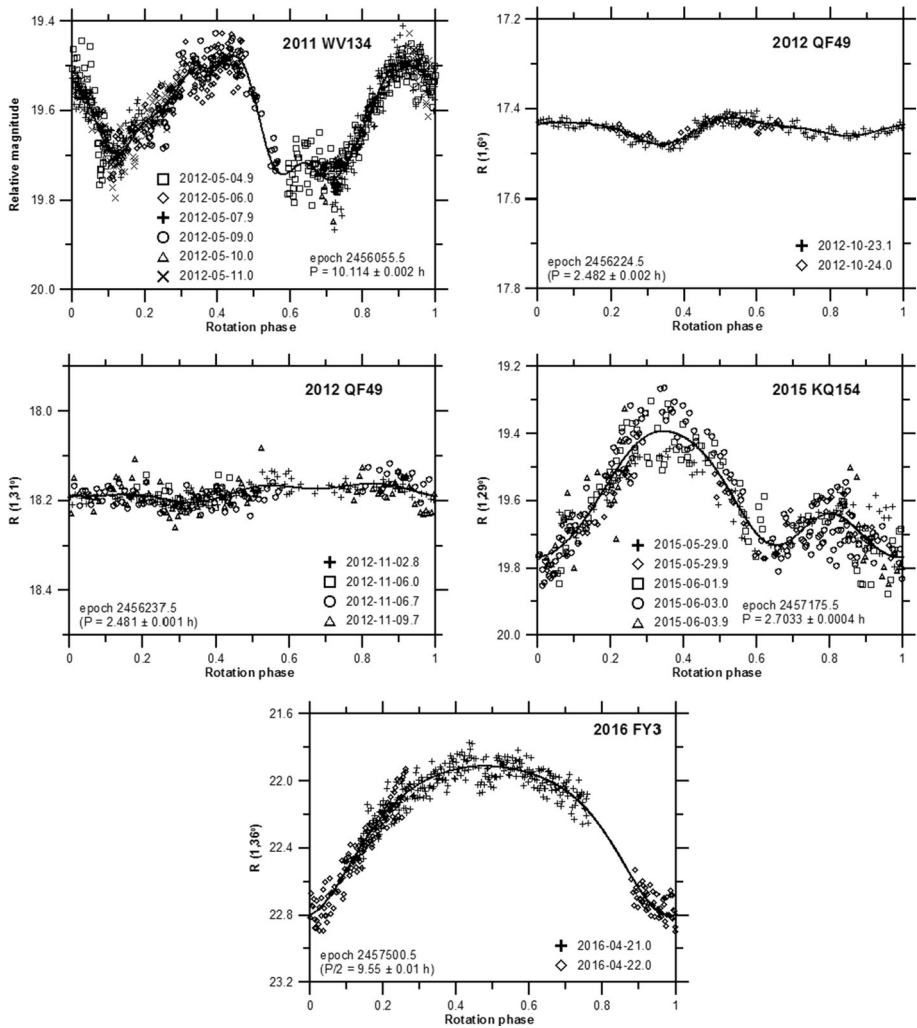
**Fig. 5** continued

## 2.5 The IAC80 0.8 m Telescope in Tenerife (OT-IAC80)

This 0.82 m $F / 11.3$ telescope was entirely built in Spain and installed in 1991 at Teide Observatory (OT) at 2390 m altitude in Tenerife, Canary Islands, Spain. At its direct Cassegrain focus the CAMELOT camera with $2048 \times 2048$ 13.5 μm pixels in installed, providing 0.304 ″/pixel and a square 10.6′ field. Up to 9 broad band or narrow band filters could be mounted in the filter wheel, and we used Harris $R$ to observe 2015 TB145. The telescope could track or guide at non-sidereal rates. The median OT site seeing is 0.8 ″, while the OT-IAC80 typical seeing is 1.0 ″.
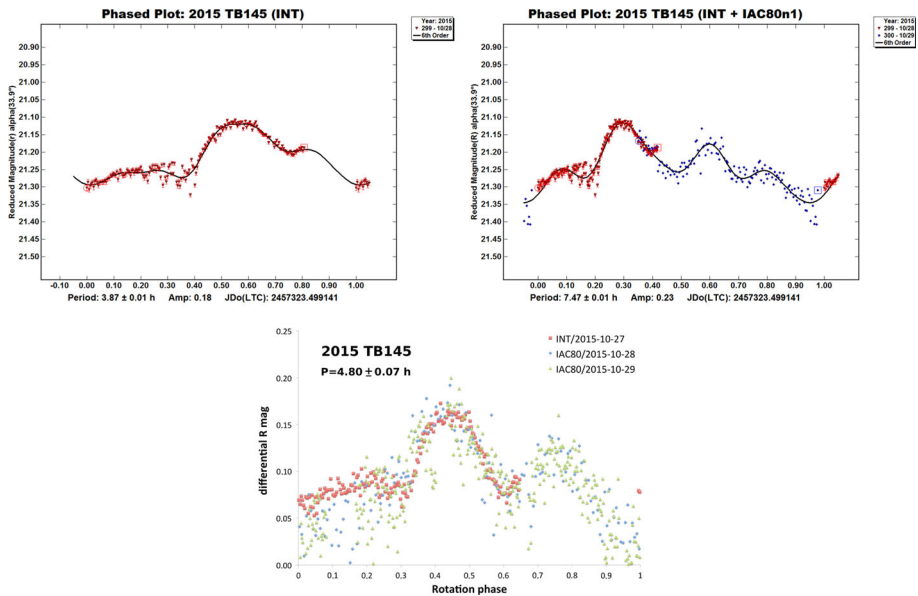
**Fig. 6** Lightcurve of PHA 2015 TB145 (the "Halloween asteroid") observed with the OT-IAC80 and ORM-INT telescopes

## 2.6 The OSN 0.9 m Telescope in Spain (OSN-T90)

This 0.91 m F/8 telescope is owned by the *Instituto de Astrofísica de Andalucía* (IAA-CSIC), being installed at the Sierra Nevada Observatory (OSN, South of Spain) at 2896 m altitude. At one of the Nasmyth foci sits the CCDT90 camera using a VersArray 2048 13.5 μm pixels CCD providing 0.387 ″/pixel and a square 13.2′ field. We observed one target in clear filter using $2 \times 2$ binning which allowed only 6 s readout in slow mode. The typical seeing in Sierra Nevada is around 1.5 ″.

## 2.7 The CTIO SMARTS 0.9 m Telescope in Chile (CTIO-T90)

This Boller and Chivens 0.9 m Cassegrain F / 13.6 telescope was installed in 1965 at Cerro Tololo Inter-American Observatory (CTIO) at 2200 m altitude in the Chilean Andes, being operated since 2009 by the North-American SMARTS universities consortium. It is equipped with the 2KCCD 2048 Tek2K detector with 24 μm pixels providing 0.4 ″/pixel and a square 25′ field. The readout time is long (53 s), but the CCD could be read using 4 amplifiers (QUAD mode) resulting in 25 s readout time and four quadrants having different levels (due to different gains) separated by the overscan vertically centered in the middle of the images. The telescope has a suite of filters from which we used Sloan r. Typical seeing in Cerro Tololo is 0.8 ″.

## 2.8 The Mercator 1.2 m Telescope in La Palma (ORM-Mer)

This 1.2 m F/8.3 telescope is operated by the Belgium Leuven University at *Roque de los Muchachos Observatory* (ORM) in La Palma, Canary Islands, Spain. At the tilted Cassegrain focus of the telescope sits the modern MAIA camera, a three-channel imager
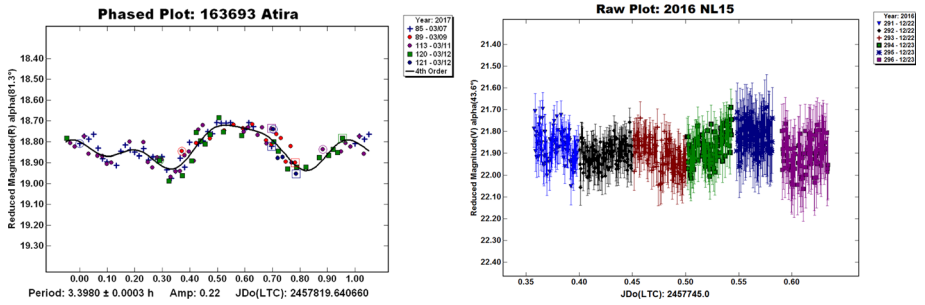
**Fig. 7** Lightcurve of NEAs observed with the OSN-T90 telescope (secured and candidate periods)
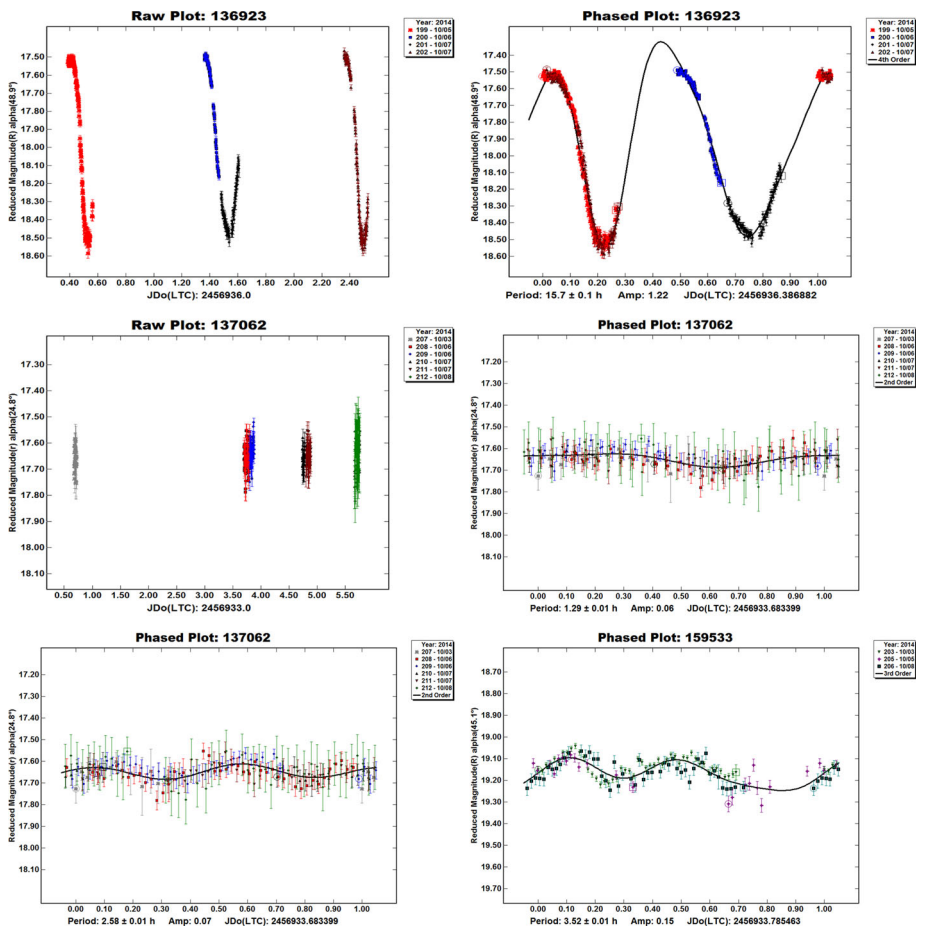


**Fig. 8** Lightcurves of NEAs observed with the CTIO-T90 telescope (secured and candidate periods)
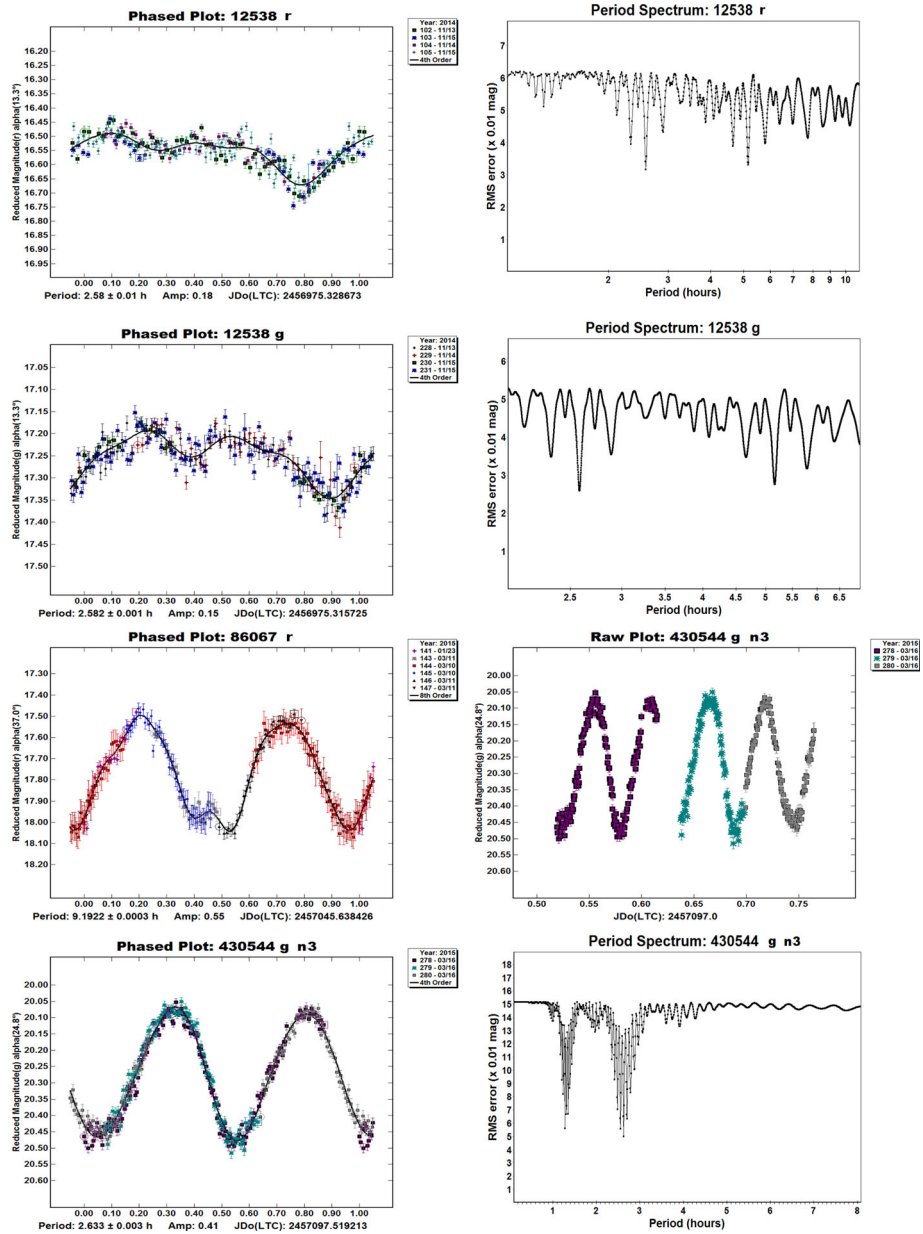
**Fig. 9** Lightcurves of NEAs observed with the ORM-Mer telescope (secured and candidate periods)

originally built for ESA's Eddington mission (later canceled), capable for simultaneous fast-cadence three-color photometry *ugr* which provides the opportunity to check for color variation along the lightcurves. The three MAIA frame-transfer CCDs consist each in 13.5 µm 2048 × 3072 pixels, at a scale of 0.28″/pixel, resulting in a rectangular 9.4′ ×
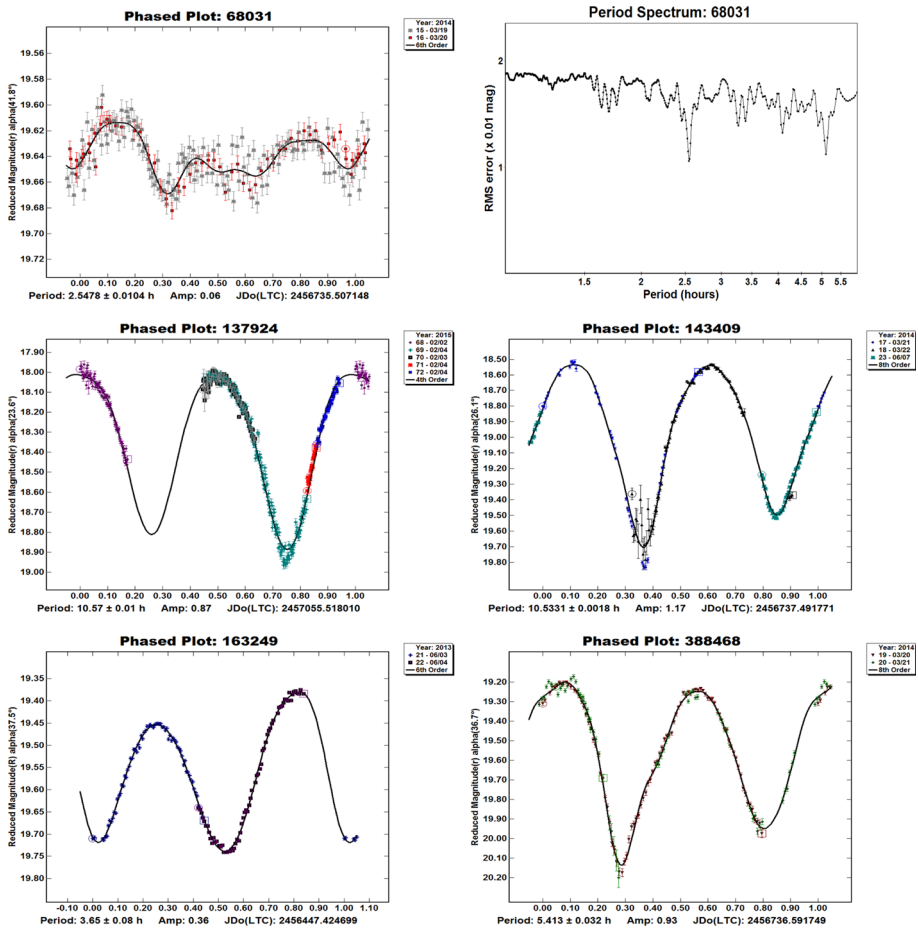
**Fig. 10** Lightcurves of NEAs observed with the ORM-INT telescope (secured and candidate periods)

14.1′ field. The Mercator telescope is capable of tracking at differential rates. The typical seeing at 2400m altitude in La Palma is 0.8″.

## 2.9 The Danish 1.5 m Telescope in Chile (LS-Dan)

This Grubb-Parsons 1.54 m $F$/4.9 Ritchey-Chretien telescope was installed in 1979 by Denmark at the European Southern Observatory La Silla (ESO), Chile. In 2012 it was refurbished by the Czech company *Projectsoft*, and during the last years it has been used in the NEOSource project (by PI: P. Pravec) for photometry of NEAs and other asteroids, being operated mostly in remote control mode from Ondřejov, the Czech Republic. The telescope is equipped with the Michelle CCD camera with 2048 24 μm pixels providing 0.37″/pixel and a square 12.6′ field. During our Chilean run we used the standard Johnson $R$ filter. The telescope is capable of tracking at differential rates. Typical seeing at 2400 m altitude in La Silla is 0.8″.
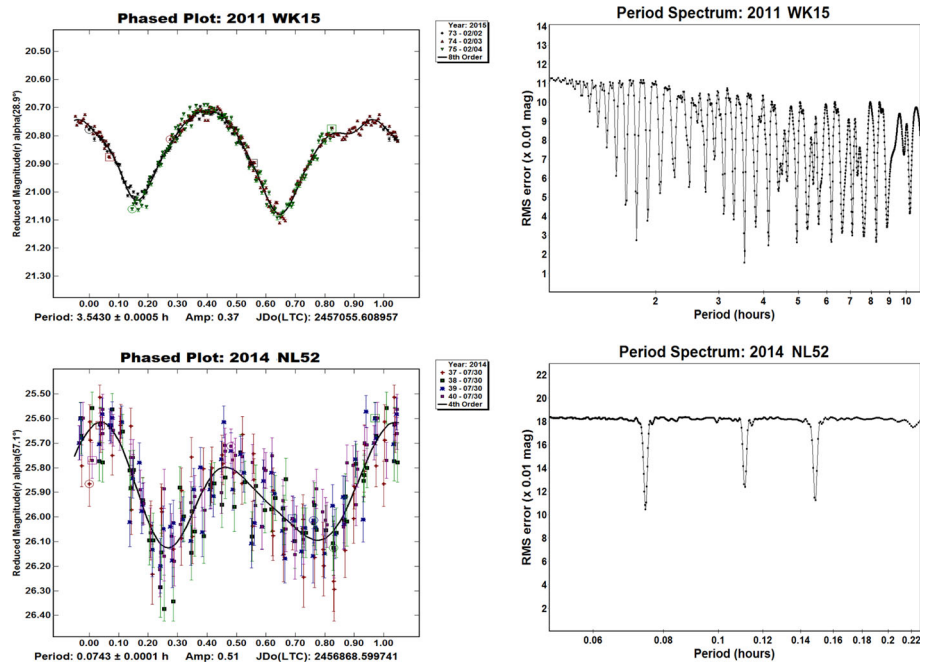
**Fig. 10** continued

## 2.10 The INT 2.5 m Telescope in La Palma (ORM-INT)

The 2.5 m Isaac Newton Telescope is owned by the Isaac Newton Group (ING), being located at 2336 m altitude at the ORM observatory in La Palma, Canary Islands, Spain. At its $F/3.3$ prime focus is located the WFC mosaic camera consisting of four CCDs 2048 13.5 μm pixels resulting in 0.33 ″/pixel and 34′ field with a missing square 12′ in its NW corner. Many broad band and narrow band filters are available, and during our runs we used mostly Sloan $r$. The telescope is capable of tracking at differential rates. For the fast moving objects we used the entire central CCD4 (22′ × 11′ field, reading each image in 48 s in slow mode or 29 s in fast mode), while for slower moving objects we window the central 10′ of CCD4 (reducing the readout to 18 s in slow mode) or to 5′ (6 s readout in slow). The median ORM site seeing is 0.8″, while the INT typical seeing is ∼ 1.2″.

## 2.11 The WHT 4.2 m Telescope in La Palma (ORM-WHT)

The 4.2 m William Herschel Telescope (WHT) is owned by the Isaac Newton Group (ING), being located at 2336 m altitude at the ORM observatory in La Palma, Canary Islands, Spain. At the tilted $F/11$ Cassegrain focus of the telescope sits the ACAM camera and low resolution spectrograph, being available for most of the nights. The ACAM pixel size is 15 μm resulting in 0.25″ scale and a circular 8′ field of view. A suite of broad band and narrow band filters are available for ACAM, and for observing 101955 Bennu we used RGO $R$, Harris $V$ and Bessel $B$ and $I$. The telescope is capable of tracking and guiding at

**Table 1** Technical characteristics of the telescopes and total observed time (ObsT column)

| Observatory | Country | Telescope | Acronym | D (m) | F/D | Camera | Pixel (") | FOV (') | Seeing (") | ObsT (h) |
|---|---|---|---|---|---|---|---|---|---|---|
| Isaac Aznar (private) | Spain | Meade 14" | IAO-T35 | 0.35 | 10 | SBIG STL1001e | 1.44 | 25 | 2.0 | 445 |
| AIRA Bucharest | Romania | Zeiss T50 | Buc-T50 | 0.50 | 10 | SBIG STL11000M | 0.25 | 16 × 11 | 3.0 | 139 |
| SpaceObs (private) | Chile | Caisey SON | SON-T50 | 0.50 | 8 | Apogee Alta U42 | 0.80 | 27.3 | 1.5 | 28 |
| Modra | Slovakia | Zeiss T60 | MOD-T60 | 0.60 | 5.5 | Apogee Ap8p | 1.50 | 25 | 3.0 | 312 |
| Teide Observatory | TF Spain | IAC80 | OT-IAC80 | 0.82 | 11.3 | CAMELOT | 0.30 | 10.6 | 1.0 | 10 |
| Sierra Nevada | Spain | T90 | OSN-T90 | 0.91 | 8 | CCDT90 | 0.39 | 13.2 | 1.5 | 16 |
| Cerro Tololo | Chile | SMARTS 0.9 | CTIO-T90 | 0.90 | 13.6 | Tek2K | 0.40 | 25 | 0.8 | 39 |
| Roque de los Muchachos | LP Spain | Mercator | ORM-Mer | 1.20 | 8.3 | MAIA | 0.28 | 9.4 × 14.1 | 0.8 | 128 |
| La Silla | Chile | Danish | LS-Dan | 1.54 | 4.9 | Michelle | 0.37 | 12.6 | 0.8 | 57 |
| Roque de los Muchachos | LP Spain | INT | ORM-INT | 2.50 | 3.3 | WFC | 0.33 | 34 | 1.2 | 100 |
| Roque de los Muchachos | LP Spain | WHT | ORM-WHT | 4.20 | 11 | ACAM | 0.25 | 8 | 1.2 | 7 |

differential rates. The measured median seeing at WHT is 0.8 ″, matching the ORM typical natural seeing.

## 3 Planning Tools and Data Reduction Software

### 3.1 Long Planning Tool

The small sizes of the majority of NEAs impose tight constraints for scheduling any lightcurve observations, the favorable geometry being usually met during Earth close approaches when the apparent magnitude typically decreases by several magnitudes. Depending of the size of these objects, the suitable intervals for photometric observations occur on average only five to ten times per century (Popescu et al. 2011).

With the purpose to optimally schedule our EURONEAR observing campaigns, we designed the public *Long Planning* web-based tool [3] which uses a simple two-body orbital model (accurate enough for this purpose) to select the observable NEAs given any particular location (MPC observatory code) and dates. The computation uses the orbital parameters provided by the ASTORB database.[4]

The input parameters of *Long Planning* are:

1. A list of asteroid designations in a plain text format, with an object designation on a new line, or the option to search for all NEAs having no lightcurve data, according to Minor Planet Center LCDB database;
2. The IAU code of the observing site;
3. The observing date and the number of subsequent nights for the campaign to perform the computation;
4. Few additional constraining parameters, namely: limiting apparent magnitude, maximum proper motion (in arcsec per minute), minimum altitude to start the observations (in degrees above the horizon) and the minimum number of hours for which the object is observable.

The result consists in a summary `html` table showed on the web-page, plus a `.csv` formatted file containing more detailed information: the time interval during which the object is observable (in hours, according to the specified inputs), the night when the object has the brightest magnitude and the best night with the highest number of hours is observable. The magnitude in these two cases is also provided. The additional output (`.csv` file) can be used for post-processing with other software (such as creating customizable graphs or pivot tables, i.e. with Excel or Open Office). It provides the magnitude, proper motion and the nightly observing window—number of hours during which the object is observable for each night in the required interval.

We do not provide any coordinates, as the two body problem is approximate—typical uncertainty for NEAs in this simple model could reach a few dozen arcminutes. For obtaining the precise ephemerides, the user should use a dedicated ephemeris service for the objects and dates included in our output list.

---

[3] http://www.euronear.org/tools/longplan.php.

[4] http://www.naic.edu/~nolan/astorb.html.

## 3.2 LiDAS Reduction Pipeline

The *Lightcurve Determination for Asteroids* (LiDAS) pipeline was written in 2014 by the EURONEAR collaborator and ING student Vlad Tudor under the guidance of Ovidiu Vaduvescu. It is aimed to offer a quick look and semi-automatic data reduction of the asteroid lightcurves during one observing session, in order to allow easy planning of future sessions (nights). LiDAS is written in Python under Linux and uses IRAF [5] and the DS9 image display. The input consists in the raw images in FITS format (science, bias and flats), while the output consists in two lightcurve plots (in png format) and the ASCII file including the time, differential magnitudes and errors (file lightcurve/final.dat). The asteroid instrumental magnitudes are calculated based on the relative flux of many stars in the field using an arbitrarily field magnitude zero point, thus no standard catalog stars is needed and there will be no apparent magnitudes in the output. The pipeline does not correct for heliocentric or geocentric distance, neither for the phase angle.

LiDAS includes six main Python modules which must be run successively. We present them here. First, the bias, flat field and science raw images must be stored in three folders (BIAS, FLAT and object1, respectively) under the main LIDAS directory. Second, the red1CCD.py module must be run for processing the raw science images. For multi-chip cameras (like the INT WFC), only the central chip imaging the target is used for calibration. Third, the aligner.py module must be run to allow manual alignment of the field, by validating the position of one arbitrary (preferably more isolated) star visible in all images. Although manual, this algorithm accommodates for any possible jumping of the telescope and also for any temporary breaks in the session due to bad weather. Fourth, the coord_finder_*.py module must be run to identify and measure the position of the asteroid in each image, based on the timing read from the header of images (in JD, MJD, BJD or other similar format). This step could be done in two possible ways: a) by running coord_finder_auto.py which assumes linear movement during the session (true in virtually all cases), measuring the asteroid position only in the first and last image, or b) by running coord_finder_man.py to manually validate the position of the asteroid in each image of the whole session. Fifth, the lightcurve.py module must be run to measure the flux automatically, the asteroid relative magnitudes and to build the asteroid lightcurve. In 2015 the new module lightcurve_psf.py was added in LiDAS to allow PSF asteroid magnitude fitting (an improved alternative to aperture photometry) by defining the asteroid pointspread function (PSF) based on stars in the current image tracked at half the asteroid proper motion. Sixth, the final lightcurve can be plotted alone using plotter.py.

In LiDAS we call the IRAF daofind task to detect stars in the first image using a threshold of 10 sigma and the value of the standard deviation of the sky, previously assessed manually. The pipeline performs aperture photometry for all detected stars in each image, by using an aperture with a diameter 3 times the full width at half maximum (FWHM, also manually assessed) and a sky annulus matching the FWHM. For each detected star, LiDAS builds individual star stellar lightcurves used to flag the star as variable or non-variable. We consider variable stars those with lightcurves containing at least one measurement which deviates by more than 2 standard deviations from its mean magnitude calculated during the entire observing session. We use all non-variable stars as

---

calibration stars for the asteroid, by subtracting in each image their mean instrumental magnitude from the instrumental magnitude of the asteroid. Finally, we normalize the asteroid lightcurve to zero. Four curves are built by LiDAS in the plotted output (see Fig. 1 for a sample): the asteroid relative magnitude (final lightcurve, panel a), the mean instrumental magnitude of the selected calibration stars (b), the instrumental magnitude of all detected stars (in different colors, c) and the asteroid instrumental magnitude (d).

### 3.3 MPO Canopus Software

The Minor Planet Observer *MPO Canopus* (hereafter Canopus) is a Windows based lightcurve measurement and analysis package developed by the American amateur astronomer Brian D. Warner at Palmer Divide Observatory.[6] The program auto-matches the detected stars in the observed fields and filters versus catalog stars taken from the built-in MPOSC3 catalog (about 300 million stars or in average 2 stars per square arcmin) or from the third party catalogs APASS, UCAC4 and USNO SA2. The measured instrumental magnitudes are transformed into reduced magnitudes using the embedded *PhotoRed* which calibrates the field using up to 5 catalog stars and corrects the color index and second order extinctions. Using the embedded StarBGone module, the software allows subtraction of stars located on the asteroid path, making it feasible for denser star fields. Canopus easily merge data from several nights and different observers and finally fits the asteroid light-curve based on the standard FALC (Fourier analysis of Lightcurves) algorithm developed by Harris et al. (1989). Besides asteroids, the software can measure lightcurves of variable stars, stars hosting exoplanets, and also it can do astrometry and search of unknown asteroids. Two comprehensive PDF manuals join the package, while a book written by the same author presents in details the theory and step by step reduction procedures (Warner 2006). To allow rapid learning by new EURONEAR lightcurve reducers, O. Vaduvescu and A. Aznar wrote a short cookbook (11 pages) detailing how to use Canopus to reduce pre-processed images.[7]

   We used Canopus for data reduction of lightcurves of most asteroids presented in this paper, except for those observed in Modra (using ALC software), Bennu (WHT, using LiDAS PSF) and 2015 TB145 (IAC80, using IRAF). Before running Canopus we used some in-house IRAF scripts correcting the raw FITS images for bias and flat field, and eventually fixing essential data in the image headers coming in different format from some telescopes. Most lightcurves could be fit by classic bimodal periods (Fourier order 2 showing two maxima in the phase curve plot) to model typical ellipsoid shapes for most targets, while few other lightcurves allowed higher orders to fit more than two maxima, due to more complicated topologies, possible binarity or phase angle circumstances. Higher orders were fitted in a prudent manner, starting from second order, then gradually increasing the order to decrease residuals.

## 4 The Observed NEAs and Results

Table 2 includes all 101 NEAs observed during our 2014-2017 campaign and a few older targets observed but not published by Modra station. We list the NEA number or designation, orbital class (APollo, AMor or ATen), absolute magnitude $H$ (according to the

---

[6] http://www.minorplanetobserver.com/MPOSoftware/MPOCanopus.htm.

[7] http://www.euronear.org/manuals/Canopus-EURONEAR-Cookbook.pdf.

**Table 2** 101 NEAs observed during the EURONEAR lightcurve survey

| NEA | Cls | H | Obs.nights | Telescope | V | μ | Exp | T | H(α) | α | B | A | P | σ | PL |
|---|---|---|---|---|---|---|---|---|---|---|---|---|---|---|---|
| 2102 Tantalus | AP | 16.0 | 01/01–17/01/17 | IAO-T35 | 14.1–16.5 | 17.8–3.0 | 240 | 27 | 18.43 | 76.9 | V | 0.06 | **2.3865** | 8e−4 | 2.384 |
| 3103 Eger | AP | 15.3 | 25/01–03/02/17 | IAO-T35 | 15.8–15.6 | 1.9–2.0 | 180 | 8 | 16.61 | 23.5 | V | 0.89 | **5.7099** | 4e−4 | 5.7059 |
| 3352 McAuliffe | AM | 15.8 | 28/11–02/12/16 | IAO-T35 | 16.3–16.4 | 8.4–4.0 | 300 | 13 | 17.03 | 20.8 | V | 0.10 | 4.504 | 2e−3 | 2.2060 |
| 5143 Heracles | AP | 14.0 | 11/11–17/11/16 | IAO-T35 | 13.5–13.0 | 3.6–6.1 | 200;70 | 26 | 16.17 | 46.6 | V | 0.19 | **2.7072** | 2e−4 | 2.7063 |
| 5587 | AM | 13.8 | 30/09–03/10/16 | IAO-T35 | 18.7 | 1.2 | 300 | 15 | 14.40 | 15.7 | R | 0.72 | **5.0524** | 7e−4 | 5.0522 |
| 5604 | AT | 17.2 | 14/03–18/03/17 | IAO-T35 | 14.4–14.9 | 2.3–1.7 | 90 | 36 | 18.86 | 37.0 | Vr | 0.20 | **5.3375** | 2e−3 | 5.3375 |
| 5836 | AM | 15.1 | 14/10–27/10/16 | IAO-T35 | 15.6–15.5 | 1.1 | 200 | 8 | 15.67 | 18.7 | V | 0.67 | **4.953** | 1e−3 | 4.9543 |
| 7341 | AP | 16.9 | 08/10–11/10/16 | IAO-T35 | 16.5–16.4 | 1.3–1.4 | 300 | 14 | 17.30 | 11.3 | R | 0.29 | **4.221** | 3e−3 | 4.2096 |
| 16834 | AP | 15.6 | 24/08–26/08/16 | IAO-T35 | 15.9 | 3.2–3.0 | 180 | 11 | 18.05 | 58.1 | V | 0.47 | **9.36** | 1e−2 | 9.345 |
| 40267 | AP | 15.4 | 13/02–15/02/17 | IAO-T35 | 15.5–15.4 | 3.6–3.4 | 240 | 10 | 16.50 | 7.2 | V | 1.07 | **4.957** | 3e−3 | 4.9567 |
| 257838 | AM | 18.2 | 09/08–23/08/16 | IAO-T35 | 17.1–17.0 | 0.8–0.9 | 240 | 24 | 19.04 | 22.0 | V | 0.53 | 10.304 | 3e−3 | 11.094 |
| 326683 | AM | 18.4 | 02/12–08/12/16 | IAO-T35 | 15.4–14.9 | 5.1–5.5 | 180 | 11 | 18.89 | 11.2 | R | 1.26 | **6.273** | 1e−3 | 6.262 |
| 347813 | AM | 17.6 | 26/08–01/09/16 | IAO-T35 | 17.1–17.2 | 2.5–2.4 | 300 | 19 | 18.95 | 21.3 | V | 0.83 | **5.914** | 1e−3 | 5.915 |
| 370307 | AM | 16.7 | 29/10–30/10/16 | IAO-T35 | 16.5 | 4.0 | 180 | 9 | 18.73 | 51.9 | R | 0.53 | **4.234** | 8e−3 | 4.218 |
| 413002 | AM | 18.8 | 04/01–06/01/17 | IAO-T35 | 17.0 | 2.5 | 300 | 11 | 20.31 | 38.9 | V | 0.29 | **4.880** | 7e−3 | 4.887 |
| 467963 | AP | 18.6 | 19/10–09/11/16 | IAO-T35 | 15.9–17.1 | 8.4–2.1 | 120 | 52 | 19.40 | 23.2 | R | 0.08 | **14.95** | 2e−2 | 15.69 |
| 468448 | AM | 17.8 | 01/08–03/08/16 | IAO-T35 | 16.5–16.4 | 1.2–1.3 | 240 | 12 | 18.55 | 16.6 | V | 0.28 | **5.330** | 7e−3 | 5.325 |
| 470510 | AM | 19.3 | 02/09–28/09/16 | IAO-T35 | 16.9–17.7 | 2.8–2.2 | 300 | 31 | 19.86 | 6.7 | R | 1.12 | **32.66** | 1e−2 | 32.26 |
| 2011 WO41 | AP | 16.6 | 17/02–25/02/17 | IAO-T35 | 17.2 | 2.2 | 180 | 29 | 17.35 | 22.9 | V | 0.14 | 5.73 | 1e−2 | 4.609 |
| 2014 KD91 | AM | 17.3 | 29/09–05/10/16 | IAO-T35 | 16.9–16.3 | 2.2–3.2 | 300 | 18 | 18.20 | 23.3 | V | 0.19 | **3.008** | 1e−3 | 2.829 |
| 2016 LX48 | AP | 19.4 | 21/09–27/09/16 | IAO-T35 | 15.5–16.1 | 7.5–3.6 | 180 | 26 | 20.22 | 47.7 | R | 0.38 | **5.669** | 2e−3 | 5.6799 |
| 2017 AC5 | AM | 17.2 | 17/03–21/03/17 | IAO-T35 | 17.8 | 2.4–2.5 | 180 | 16 | 20.75 | 5.6 | V | 0.75 | **5.9348** | 2e−3 | – |
| 2017 BQ6 | AP | 21.4 | 30/01–02/02/17 | IAO-T35 | 16.6–15.8 | 5.0–10.8 | 30 | 3 | 23.00 | 32.7 | V | 0.38 | **2.150** | 1e−3 | – |
| 9400 | AM | 14.9 | 13/09–06/10/15 | Buc-T50 | 15.2–14.9 | 3.9–5.3 | 60 | 54 | 16.30 | 37.2 | W | 0.47 | 82.6 | 1e−1 | 97.1 |
| 85989 | AT | 17.1 | 07/07–19/07/15 | Buc-T50 | 15.9–13.9 | 2.0–12.0 | 60;30;20 | 41 | 19.13 | 46.0 | W | 1.30 | 7.6611 | 3e−4 | 7.6638 |
| 285944 | AM | 16.5 | 20/08–24/08/14 | Buc-T50 | 13.2–14.5 | 17.7–7.8 | 70;10;15 | 14 | 18.42 | 44.5 | W | 0.09 | TP | – | 2.2455 |

**Table 2** continued

| NEA | Cls | H | Obs.nights | Telescope | V | μ | Exp | T | H(α) | α | B | A | P | σ | PL |
|---|---|---|---|---|---|---|---|---|---|---|---|---|---|---|---|
| 348400 | AM | 17.3 | 23/07-25/07/15 | Buc-T50 | 14.7-14.5 | 1.8-2.2 | 60 | 8 | 18.31 | 34.0 | W | 0.11 | 2.43 | 7e-2 | 2.4149 |
| 363814 | AM | 18.0 | 11/07-13/07/16 | Buc-T50 | 15.6-15.5 | 9.4-10.5 | 20 | 11 | 18.57 | 7.1 | W | 0.07 | TP | - | - |
| 214088 | AP | 15.3 | 25/06-03/07/14 | SON-T50 | 16.6 | 1.4-1.3 | 90 | 28 | 15.75 | 15.4 | W | 0.30 | **6.336** | 1e-3 | 6.342 |
| 7350 | AP | 17.3 | 03/04-20/04/16 | Mod-T60 | 16.0-16.6 | 5.8-3.0 | 30;40;60 | 38 | 18.90 | 58 | W | 0.27 | **3.58264** | 9e-5 | 3.580 |
| 9950 ESA | AM | 16.2 | 22/08-03/09/13 | Mod-T60 | 16.8-16.8 | 2.2-1.8 | 40;60 | 26 | - | 60 | W | 0.89 | 6.7078 | 7e-4 | 6.712 |
| 17188 | AP | 16.5 | 27/06-01/07/13 | Mod-T60 | 14.6-15.1 | 3.9-2.6 | 40 | 15 | 17.32 | 23 | W | 0.45 | **5.0638** | 8e-4 | 5.352 |
| 21374 | AM | 17.4 | 17/04/14 | Mod-T60 | 16.9 | 1.3 | 60 | 3 | 19.02 | 53 | W | 0.07 | TP | - | 3.405 |
| 68267 | AP | 16.9 | 11/10-14/10/14 | Mod-T60 | 15.7-15.8 | 13.8-8.7 | 15;18;25 | 6 | 20.10 | 97 | W | 0.17 | TP | - | - |
| 68348 | AP | 14.3 | 07/07-11/07/11 | Mod-T60 | 15.1-15.0 | 4.0-4.4 | 30 | 20 | 15.42 | 47 | W | 0.16 | **3.3313** | 3e-4 | 3.324 |
| 85713 | AP | 15.5 | 02/11-15/11/06 | Mod-T60 | 15.1 | 5.5-9.0 | 30 | 5 | - | 10 | W | 0.12 | TP | - | 5.370 |
| 138127 | AT | 17.1 | 09/03-20/03/14 | Mod-T60 | 16.0-16.5 | 7.4-5.1 | 30;35 | 16 | 19.44 | 81 | W | 0.20 | **2.5904** | 1e-4 | 2.586 |
| 141354 | AM | 17.4 | 30/04-08/06/16 | Mod-T60 | 15.8-16.9 | 2.2-0.5 | 90;120;180 | 38 | 18.63 | 40 | W | 0.35 | 10.784 | - | 19.76 |
| 153951 | AM | 18.6 | 30/01/12 | Mod-T60 | 16.9 | 2.2 | 120 | 4 | - | 4 | W | 0.73 | 6.9 | 1e-1 | 7.072 |
| 170502 | AP | 17.2 | 05/12/11 | Mod-T60 | 14.7 | 16.2 | 30 | 3 | - | 45 | W | 0.37 | TP | - | - |
| 192642 | AP | 16.3 | 11/02/12 | Mod-T60 | 15.4 | 1.7 | 60 | 3 | 16.14 | 4 | W | 0.08 | TP | - | 17.08 |
| 242708 | AP | 18.1 | 19/05-07/06/14 | Mod-T60 | 16.2-16.6 | 16.5-3.2 | 15;60;70 | 9 | 20.01 | 57 | W | 1.03 | TP1 | - | 4.289 |
| 251346 | AP | 17.2 | 16/11/13 | Mod-T60 | 16.2 | 1.3 | 60 | 3 | 21.16 | 139 | W | 0.67 | 2.72 | - | 2.718 |
| ... | ... | 17.2 | 10/01-12/01/14 | Mod-T60 | 15.7-16.1 | 5.9-7.5 | 20 | 3 | 21.15 | 119 | W | 0.11 | **2.719** | - | ... |
| 361071 | AM | 15.4 | 15/08-18/08/13 | Mod-T60 | 14.9 | 5.4-5.3 | 30 | 13 | 17.21 | 51 | W | 0.33 | **4.0888** | 4e-4 | 4.093 |
| 387733 | AT | 19.0 | 11/04-16/04/14 | Mod-T60 | 14.6-15.0 | 7.0-6.4 | 20;30 | 17 | 19.45 | 20 | W | 0.11 | **2.4686** | 2e-4 | 2.467 |
| 388945 | AP | 20.4 | 28/04-29/04/16 | Mod-T60 | 15.2-15.0 | 10.8-12.7 | 20;15 | 3 | 21.17 | 27 | W | 0.15 | TP | - | 44.2 |
| 450160 | AP | 16.7 | 24/03-26/03/16 | Mod-T60 | 16.4-16.5 | 9.9-8.9 | 20;24 | 4 | 18.30 | 60 | W | 0.26 | TP | - | 14.51 |
| 2005 TF | AM | 20.2 | 14/11/16 | Mod-T60 | 16.3 | 3.9 | 30 | 11 | 20.85 | 17 | W | 0.22 | **2.724** | 5e-3 | 2.57 |
| 2009 DO111 | AP | 22.8 | 16/03/09 | Mod-T60 | 15.4 | 5.1 | 15 | 6 | - | 18 | W | 0.41 | **0.0488781** | 7e-7 | 0.04890 |
| 2010 RF181 | AM | 20.7 | 19/11/10 | Mod-T60 | 15.1 | 8.5 | 25 | 3 | - | 10 | W | 0.05 | 4.6 | - | - |
| 2011 MD | AM | 28.0 | 24/06-26/06/11 | Mod-T60 | 18.3-18.1 | 11.2-10.0 | 22;14;5 | 3 | 29.92 | 64 | W | 0.73 | 0.38733 | 2e-5 | 0.1937 |

**Table 2** continued

| NEA | Cls | $H$ | Obs.nights | Telescope | $V$ | $\mu$ | Exp | $T$ | $H(\alpha)$ | $\alpha$ | $B$ | $A$ | $P$ | $\sigma$ | PL |
|---|---|---|---|---|---|---|---|---|---|---|---|---|---|---|---|
| 2011 WV134 | AP | 17.2 | 04/05–10/05/12 | Mod-T60 | 15.4–15.3 | 8.3–6.0 | 20;25;30 | 23 | – | 86 | W | 0.28 | **10.114** | 2e−3 | 10.105 |
| 2012 QF49 | AM | 17.4 | 22/10–09/11/12 | Mod-T60 | 14.9–16.1 | 6.1–4.6 | 15;20;30 | 12 | 17.75 | 15 | W | 0.05 | **2.482** | 2e−3 | – |
| 2014 CU13 | AP | 21.9 | 06/03–08/03/14 | Mod-T60 | 16.8–16.1 | 11.3–28.6 | 20;10 | 3 | 22.65 | 27 | W | 0.30 | TP | – | 14.36 |
| 2015 KQ154 | AM | 18.8 | 28/05–03/06/15 | Mod-T60 | 16.3–16.8 | 8.3–6.9 | 15 | 12 | 19.60 | 29 | W | 0.37 | 2.7033 | 4e−4 | 6.97 |
| 2016 FY3 | AP | 21.3 | 20/04–21/04/16 | Mod-T60 | 16.6–16.1 | 8.5–13.5 | 30;20 | 10 | 22.35 | 36 | W | 0.89 | 19.1 | 2e−2 | 19.8 |
| 163693 Atira | AT | 16.3 | 07/03–12/03/17 | OSN-T90 | 17.0–17.1 | 1.1 | 200 | 9 | 18.88 | 81.3 | R | 0.22 | **3.3980** | 3e−4 | 3.3984 |
| 2016 NL15 | AP | 20.0 | 22/12/16 | OSN-T90 | 16.7 | 11.0 | 30 | 7 | 23.15 | 47.5 | R | 0.55 | **23.22** | 1e−2 | 23.22 |
| ... | ... | ... | 19/12–25/12/16 | IAO-T35 | 16.9–9.4 | 12.6–9.4 | 42 | 12 | ... | ... | V | ... | ... | ... | ... |
| 136923 | AM | 16.3 | 05/10–07/10/14 | CTIO-T90 | 16.5 | 2.6 | 50 | 15 | 18.05 | 48.9 | R | 1.22 | 15.7 | 1e−1 | – |
| 137062 | AP | 16.6 | 05/10–07/10/14 | CTIO-T90 | 17.5 | 1.9 | 60 | 15 | 17.65 | 24.8 | R | 0.07 | 2.58 | 1e−2 | – |
| 159533 | AM | 17.6 | 02/10–07/10/14 | CTIO-T90 | 17.5–17.4 | 0.6–0.8 | 150 | 9 | 19.17 | 45.1 | R | 0.15 | 3.52 | 1e−2 | 3.660 |
| 2015 TB145 | AP | 20.0 | 28/10–29/10/15 | OT-IAC80 | 15.2–13.8 | 2.9–10.1 | 90;15 | 10 | – | – | R | 0.16 | **4.80** | 7e−2 | 2.938 |
| ... | ... | ... | 27/10/15 | ORM-INT | 16.4 | 1.0 | 40 | 3 | 21.21 | 33.9 | r | 0.18 | TP | – | ... |
| ... | ... | ... | 28/10–31/10/15 | Buc-T50 | 15.2–15.7 | 2.8–42.6 | 40;60;70 | 11 | – | – | W | – | – | – | ... |
| ... | ... | ... | 30/10/15 | IAO-T35 | 14.2–14.1 | 7.8–8.5 | 185 | 4 | – | – | V | – | – | – | ... |
| 12538 | AP | 15.8 | 13/11–15/11/14 | ORM-Mer | 18.0 | 1.2 | 120 | 12 | 16.60 | 13.3 | r+g | 0.18 | **2.582** | 1e−3 | 5.154 |
| 27346 | AM | 15.9 | 13/03/15 | ORM-Mer | 18.7 | 2.5 | 120 | 2 | 17.50 | 45.3 | r+g | 0.08 | TP2 | – | – |
| 86067 | AM | 16.4 | 22/01–23/01/15 | ORM-Mer | 18.4 | 1.6 | 120 | 7 | 17.78 | 37.0 | r+g | 0.55 | **9.1922** | 3e−4 | 9.196 |
| ... | ... | ... | 09/03–10/03/15 | ORM-Mer | 18.3 | 1.2 | 120 | 15 | 17.38 | 23.2 | r+g | 0.57 | 9.200 | 7e−3 | ... |
| 90416 | AP | 18.7 | 22/01–24/01/15 | ORM-Mer | 16.9–16.8 | 1.9–2.0 | 60 | 8 | 19.98 | 20.3 | r+g | 0.10 | TP | – | 43.58 |
| 112985 | AM | 15.8 | 11/03/15 | ORM-Mer | 19.3 | 0.7 | 120 | 2 | 16.19 | 25.4 | r+g | 0.11 | TP2 | – | 4.787 |
| 175114 | AP | 16.6 | 13/11–14/11/14 | ORM-Mer | 16.2 | 2.1–2.0 | 90 | 7 | 17.47 | 17.4 | r+g | 0.12 | TP | – | 8.879 |
| 275976 | AP | 16.2 | 22/01–25/01/15 | ORM-Mer | 18.3–18.4 | 1.0 | 120 | 17 | 16.94 | 24.7 | r+g | 0.19 | TP | – | – |
| 285625 | AM | 17.8 | 13/03–14/03/15 | ORM-Mer | 18.8 | 0.7 | 120 | 7 | 18.32 | 8.3 | r+g | 0.06 | TP2 | – | – |
| 322763 | AP | 17.0 | 09/03–11/03/15 | ORM-Mer | 18.5 | 2.5–2.4 | 90 | 11 | 18.35 | 39.5 | r+g | ~0.10 | TP | – | – |
| 410195 | AM | 18.4 | 13/11–15/11/14 | ORM-Mer | 17.3 | 0.2 | 120 | 7 | 18.75 | 15.4 | r+g | >0.15 | TP | – | 48.05 |

**Table 2** continued

| NEA | Cls | H | Obs.nights | Telescope | V | μ | Exp | T | H(α) | α | B | A | P | σ | PL |
|---|---|---|---|---|---|---|---|---|---|---|---|---|---|---|---|
| 423747 | AM | 18.9 | 11/03–14/03/15 | ORM-Mer | 17.5–17.4 | 4.9 | 60 | 9 | 19.77 | 21.3 | r+g | 0.06 | TP | – | – |
| 425713 | AM | 19.6 | 11/03–12/03/15 | ORM-Mer | 18.6 | 1.2 | 120 | 9 | 20.60 | 24.8 | r+g | 0.29 | TP | – | 6.010 |
| 430544 | AP | 18.6 | 13/03–15/03/15 | ORM-Mer | 16.8–16.9 | 7.1–6.1 | 60 | 7 | 19.80 | 30.6 | r+g | 0.41 | **2.633** | 3e−3 | 2.630 |
| 2014 QK434 | AP | 19.1 | 22/01–24/01/15 | ORM-Mer | 17.6–17.8 | 3.5–3.3 | 45 | 8 | 20.49 | 40.4 | r+g | 0.09 | TP | – | 78.4 |
| 39796 | AM | 15.8 | 05/11/14 | LS-Dan | 16.8 | 0.8 | 150 | 9 | 16.07 | 18.9 | R | >0.10 | TP | – | 223.5 |
| 86326 | AM | 17.3 | 05/11–06/11/14 | LS-Dan | 18.2–18.1 | 2.0 | 60;55 | 18 | 19.10 | 56.4 | R | 0.08 | TP | – | 6.36 |
| 399307 | AM | 18.9 | 29/09–01/10/14 | LS-Dan | 18.0–18.1 | 0.8–0.7 | 150 | 15 | 19.05 | 7.5 | R | 0.3–0.4 | TP | – | 3.4807 |
| 408980 | AP | 18.7 | 29/09–01/10/14 | LS-Dan | 18.1 | 2.9–2.7 | 40 | 9 | 18.30 | 4.7 | R | ~0.10 | TP | – | 16.21 |
| 2014 SS1 | AM | 21.7 | 29/09–30/09/14 | LS-Dan | 17.8–17.9 | 1.0–0.9 | 30;40 | 6 | 22.63 | 34.7 | R | ~0.25 | TP | – | 16.63 |
| 24443 | AP | 16.4 | 29/07+31/07/ 14 | ORM-INT | 18.2 | 1.7 | 60 | 6 | 17.88 | 44.3 | r | 0.19 | TP | – | 4.069 |
| 68031 | AM | 18.1 | 18/03–19/03/14 | ORM-INT | 17.7 | 0.7–0.6 | 120;150 | 9 | 19.64 | 41.8 | r | 0.06 | 2.55 | 1e−2 | 4.45 |
| 137924 | AT | 17.2 | 01/02/15 | ORM-INT | 17.0 | 4.4 | 50 | 3 | 18.47 | 23.6 | r | 0.87 | **10.57** | 1e−2 | 10.570 |
| 143409 | AM | 17.9 | 20/03–21/03/14 | ORM-INT | 17.3–17.2 | 1.5 | 120 | 12 | 19.16 | 26.1 | r | 1.17 | **10.533** | 2e−3 | 10.531 |
| ... | ... | ... | 07/06/14 | ORM-INT | 17.9 | 0.8 | 120 | 2 | ... | 28.4 | r | ... | ... | ... | ... |
| 162980 | AP | 16.7 | 08/06/14 | ORM-INT | 18.2 | 1.0 | 120 | 6 | 18.73 | 54.3 | r | 0.21 | TP | – | 12.71 |
| 163249 | AP | 18.7 | 03/06/13 | ORM-INT | 16.4 | 3.8 | 30 | 3 | 19.57 | 37.5 | R | 0.35 | **3.94** | 3e−2 | 3.7663 |
| 337866 | AM | 18.8 | 28/12/15 | ORM-INT | 15.2 | 4.0 | 30 | 4 | 19.29 | 21.2 | r | 0.10 | TP | – | 8.955 |
| 377732 | AP | 17.0 | 29/07/14 | ORM-INT | 18.1 | 1.4 | 90 | 2 | 17.34 | 5.9 | r | 0.06 | TP2 | 1e−3 | – |
| 388468 | AM | 18.3 | 19/03–20/03/14 | ORM-INT | 18.1 | 1.0 | 120 | 10 | 19.67 | 36.7 | r | 0.93 | **5.41** | 3e−2 | 5.41403 |
| 391033 | AM | 19.1 | 08/06–09/06/14 | ORM-INT | 17.3 | 1.0 | 120 | 6 | 19.97 | 21.2 | r | 0.03 | TP2 | – | 850 |
| 410088 | AP | 18.1 | 02/02–03/02/15 | ORM-INT | 17.2 | 3.9–3.8 | 60 | 8 | 19.38 | 44.0 | r | 0.09 | TP | – | 4.781 |
| 411280 | AM | 19.2 | 20/02/14 | ORM-INT | 17.9 | 0.6 | 120 | 4 | 19.78 | 12.0 | r | 0.02 | – | – | 7.79 |
| 415986 | AM | 18.1 | 01/02/15 | ORM-INT | 18.7 | 1.8 | 90 | 1 | 20.05 | 40.6 | R | ~0.3 | – | – | – |
| 416151 | AP | 20.6 | 01/02/15 | ORM-INT | 17.7 | 3.6 | 60 | 4 | 21.76 | 38.8 | R | ~0.5 | TP | – | 12.191 |
| 427684 | AT | 20.2 | 28/02/15 | ORM-INT | 17.6 | 5.0 | 25 | 3 | 20.61 | 5.0 | r | >0.1 | TP | – | 8.962 |

**Table 2** continued

| NEA | Cls | H | Obs.nights | Telescope | V | $\mu$ | Exp | T | H($\alpha$) | $\alpha$ | B | A | P | $\sigma$ | PL |
|---|---|---|---|---|---|---|---|---|---|---|---|---|---|---|---|
| 429584 | AP | 19.9 | 27/02+01/03/15 | ORM-INT | 18.5–18.6 | 1.7-1.6 | 30;80 | 5 | 20.12 | 6.3 | r | ~0.3 | – | – | 43.5 |
| 2011 WK15 | AM | 19.7 | 01/02-03/02/15 | ORM-INT | 16.6 | 4.7–4.9 | 40 | 8 | 20.85 | 28.9 | r | 0.37 | **3.5430** | 5e−4 | 3.541 |
| 2013 AV60 | AP | 18.6 | 28/12/15 | ORM-INT | 17.5 | 5.9 | 40 | 2 | 20.11 | 46.5 | r | 0.22 | TP | – | – |
| 2014 NL52 | AP | 23.6 | 29/07/14 | ORM-INT | 20.8 | 2.0 | 20 | 2 | 25.86 | 57.1 | r | 0.51 | **0.0743** | 1e−4 | – |
| 101955 Bennu | AP | 20.2 | 29/08/11 | ORM-WHT | 19.9 | 4.7 | 30 | 3 | ... | 61.1 | VR | ~0.3 | ... | ... | ... |
| ... | ... | ... | 13/09/11 | ORM-WHT | 20.2 | 5.1 | 20 | 2 | 23.32 | 86.6 | BVRI | 0.43 | TP | – | 4.2968 |
| ... | ... | ... | 04/11/11 | ORM-WHT | 21.8 | 2.4 | 45 | 2 | ... | 95.6 | R | 0.31 | ... | ... | ... |

Please see Sect. 4 for the explanation of the columns

EARN database[8]) the observing date or interval (in format DD/MM/YY), telescope, apparent magnitude $V$ (according to MPC ephemerides), proper motion $\mu$ (in $''$/min), exposure time (in seconds), total observed time (in hours), reduced magnitude $H(\alpha)$ at observed phase angle $\alpha$ (in degrees), observing bands (filters), measured amplitude, derived rotation period $P$ (in hours) and the Fourier fit error $\sigma$ in the second last column.

The majority of NEAs (except for most IAO-T35 and some of MOD-T60 targets) were not observed before, and had no published periods by the date of our observations. During our survey, Brian Warner targeted many common NEAs and published his results in Minor Planet Bulletin, sometime in collaboration with other observers and once with two of us (A. Aznar and A. Sota, for the NEA 2016 NL15). For comparison with our results, we include the published literature periods (*PL*) in the last column of our Table 2, according to the ALCDEF database[9] retrieved on 15 Feb 2017 (the Period column in the object Summary pages).

We provide in the $P$ column of Table 2 the periods in three notations, depending on the uncertainty of our results. First, with bold characters we give the *secured periods* for best observed objects (most of them which agree well with published periods, and few others different). Second, we list with normal characters the *candidate periods* for incompletely covered targets, possibly dual periods (typically half or double our preferred or previously published value) or the suggested short periods for candidate tumblers. Third, we mark by *TP* the *tentative periods* for the insufficiently observed targets (sometimes given as an interval or constrained by a lower limit) and some suggested periods for objects showing multiple (more than two) solutions.

18 targets had no published periods, namely: 2017 AC5, 2017 BQ6 (observed with IAO-T35); 363814 (Buc-T50); 68267, 170502, 2010 RF181 and 2012 QF49 (MOD-T60); 136923 and 137062 (CTIO-T90); 27346, 275976, 285625, 322763 and 423747 (ORM-Mer); 377732, 415986, 2013 AV60 and 2014 NL52 (ORM-INT). We solved the period for 13 targets without known rotations and have provided constraints for other 4 targets.

We present the photometry plots in two main groups: the resolved objects (having derived secured or candidate periods) with phase Fourier fits included in the main paper in Figs. 2, 3, 4, 5, 6, 7, 8, 9 and 10, and the poorly observed objects (having derived tentative, candidate periods or no periods) including raw JD plots and some tentative fits in the Appendix in Figs. 12, 13, 14, 15, 16 and 17. In both groups the figures follow the target order presented in Table 2 listed based on the observing facility (presented in Sect. 2). For each telescope we order the targets following their number or designation.

The magnitude uncertainties are dominated by the field zero points derived from maximum 5 catalog stars in Canopus, typically bellow 0.02 mag and depending on the catalog (SDSS9 best or APASS9 whenever available, both queried manually in VizieR, otherwise MPOSC3 embedded in Canopus). The period fit uncertainties are listed from Canopus, and they should be regarded with caution, typically these being larger especially for short coverage. We will discuss next all targets, classifying our findings in 7 sub-sections.

## 4.1 Secured Periods

We accurately resolved 45 rotation periods ($P$ given in bold in Table 2) proposed to be flagged with quality codes[10] $U \sim 3$. Most of our results agree well with the data available in

---

the literature (to compare with *PL* column in Table 2), while some improve past findings. To keep the list short, we will only include references for the candidate and tentative periods, all others could be found in the ALCDEF or NEODyS databases.

Particularly, the private IAO-T35 facility was extremely productive (Fig. 2), resolving the following 20 targets: 2102 Tantalus, 3103 Eger, 5143 Heracles, 5587, 5604 (observed in two bands), 5836, 7341, 16834, 40267, 326683, 347813, 370307, 413002, 467963, 468448, 470510 (to be discussed later), 2014 KD91, 2016 LX48, 2017 AC5 and 2017 BQ6 (both with no published data). Next, MOD-T60 station secured 11 targets (Fig. 5): 7350, 17188, 68348, 138127, 251346, 361071, 387733, 2005 TF, 2009 DO111 (very fast rotator), 2011 WV134 and 2012 QF49 (not observed before). The ORM-INT secured only 6 targets (Fig. 10), mainly due to the limited time available during the runs: 137924, 143409 (both slow rotators and marginally undersampled), 163249, 388468, 2011 WK15 and 2014 NL52 (a very faint fast rotator and special target to be discussed later). Next, the ORM-Mer secured 3 targets (Fig. 9): 12538 (halving past published value of B. Warner), 86067 (observed during two runs) and 430544. Four other telescopes secured one target each: Buc-T50 - 85989 (Fig. 3), SON-T50 - 214088 (Fig. 4), OT-IAC80 - 2015 TB145 (Fig. 6) and OSN-T90 secured 163693 Atira (Fig. 7, to be discussed later).

## 4.2 Candidate Periods

We obtained good fits, considered as candidate periods, for 16 targets (*P* given in normal notation in Table 2) proposed to be flagged with quality codes $U \sim 2$. Some of them lack complete coverage, while others should be regarded as our primary solution *T*1, besides other possible dual or multiple solutions.

IAO-T35 produced 3 candidate periods. 3352 McAuliffe resulted in $P = 4.504$ h which is double of past published results $P = 2.2060$ h of Warner (2012) and other two authors. In Fig. 2 we include our fit and period spectrum. 257838 shows some mismatch in the first maximum but results in a good fit $P = 10.304$ h, which is quite close to the adopted $P = 11.094$ h of Warner (2017a) and another similar result of P. Pravec in 2000. 2011 WO41 will be discussed later.

Buc-T50 station observed 2 candidate periods (Fig. 3): 9400 and 348400, to be discussed later.

MOD-T60 station produced 7 candidate periods (Fig. 5). Although 9950 ESA shows imperfect overlay of the first night, its final fit $P = 6.7078$ h matches the literature $P = 6.712$ h by Warner (2014e). 141354 was affected by scatter due to poor weather but could be fit by $P = 10.784$ h which matches about half of the published period $P = 19.76$ h U $= 2+$ observed one month before in better amplitude conditions by Warner (2016a). 153951 could be covered fully or half period, but its fit $P = 6.9$ h matches published results $P = 7.072$ h U $= 3$ of B. Warner (according to ALCDEF). 2010 RF181 probably samples about half the period $P = 4.6$ h and has no other published data. 2011 MD is a fast rotator with dual solutions from which we prefer the longer $P = 0.38733$ h which does not match three ALCDEF references (including the adopted $P = 0.1937$ h U $= 3$ observed by B. Skiff in 2011), but it matches other two results by Franco and Apitzsch (2011) listed in the ALCDEF database. 2015 KQ154 resulted in a good fit $P = 2.7033$ h which does not match the suggested result of B. Warner P $= 6.97$ h U $= 2$ listed in ALCDEF (not published). Despite its very small amplitude, 2012 QF49 resulted in the preferred period $P = 2.482$ h. (independently from two runs), plus another possible solution, and has not been observed previously. Finally, 2016 FY3 was covered only half and our derived fit during the two nights. The plot in Fig. 5 was built to fit *P*/2

assuming symmetrical shape of the lightcurve with two maxima and two minima and consequently we derive $P = 19.1$ h which is closed to the ALCDEF period $P = 19.8$ h of B. Warner U = 3 (apparently not published).

ORM-INT generated one candidate period (Fig. 10), namely 68031 which was apparently covered during both nights. Despite its very small amplitude, we could fit a candidate period $P = 2.55$ h which is about half the published value of B. Warner $P = 4.45$ h which is very uncertain U = 1 (Warner 2014a).

CTIO-T90 produced 3 candidate periods (Fig. 8). 136923 has a very large amplitude (1.1 mag, trace of a very elongated object) not published before. We observed it for three nights during descending slope, apparently covering both its maximum and minimum. All three maxima look quite similar, probably affected by the larger phase angle (49 degrees), but apparently the data taken during the second night shows a smaller amplitude and a minimum slightly different in shape than the other two minima, thus the bimodal fit $P = 15.7$ h represents our candidate solution. 137062 was not observed before, being a low amplitude target with a dual period from which we trust the longer value $P = 2.58$ h. In Fig. 8 we include its raw JD plot followed by the two fits. 159533 was marginally undersampled but could be fit with $P = 3.52$ h which matches the shorter preferred published period $P = 3.660$ h U = 2 of Warner (2015b).

Finally, the OSN-T90 and OIA-T35 stations constrained data taken by B. Warner, being essential to solve the quasi-diurnal period of 2016 NL15 $P = 23.22$ h (Warner et al. 2017) (Fig. 7).

## 4.3 Poorly Observed Objects

Tentative fits were obtained for 32 targets insufficiently observed, very slow rotators, having very small amplitude, very low signal to noise ratios or in bad weather conditions, while lightcurves for 3 other targets could not be fitted. We discuss in this section their tentative periods or limits, marking their $P$ with $TP$ (tentative period) in Table 2 and including their plots in the Appendix (Figs. 12, 13, 14, 15, 16, 17). All these tentative periods should be regarded with caution, probably corresponding to uncertainties $U \sim 1$.

MOD-T60 generated 9 tentative fits for the following targets (plots in Appendix Fig. 13): 21374 was a low amplitude sparsely sampled object whose spin can be tentatively fit with $TP = 2.4$ h. This does not match the adopted $P = 3.405$ h U = 2 of Warner (2014b) but comes very close to $P = 2.292$ h U = 2+ of Carbognani (2014). The 68267 data seems quite noisy during two nights and could be tentatively fit with $TP = 3.5$ h, and it was not published before. 85713 was marginally under-sampled, being observed in alternance with another object. We could tentatively fit $TP = 5.398$ h, which comes close to the value $P = 5.370$ h of Warner (2015o). 170502 was insufficiently observed and has no published data, so we could only guess $TP \sim 3.6$ h. 192642 was insufficiently observed and suggests $TP = 8.54$ h which is about half the published period $P = 17.08$ h U = 2 of Warner and Megna (2012). 242708, 388945 and 2014 CU13 will be discussed later, being known as tumbler candidates. 450160 (2000 RM12) was insufficiently observed and very scattered, and we suggest $TP = 7.2$ h which is half of the adopted $P = 14.51$ h U = 2+ by Warner (2016b).

ORM-Mer produced tentative periods for 11 objects (Appendix Fig. 14). 27346, 112985 and 285625 were insufficiently observed to cover the main period, nevertheless apparently we evidenced their possible binary or tumbling nature, and they will be discussed later. 90416 had a low amplitude and not enough coverage, few possible solutions being possible following our tentative $TP = 5.3 \pm 0.1$ h which is way bellow the adopted value

$P = 43.58$ h U $= 2+$ of Warner (2015c). 175114 was insufficiently covered and shows few possible minima in the spectrum; we could only give minimum constraint $TP > 4$ h. Its adopted ALCDEF period is $P = 8.879$ h U $= 2+$ by B. Warner (ALCDEF database) which matches one minima in our spectrum. 275976 was observed during 4 nights and probably has a long period, showing clear variation during last two nights, nevertheless it was insufficiently coveraged. A tentative fit could be $TP = 6.66 \pm 0.02$ h which should be regarded with prudence. It has no published data. 322763 had a small amplitude and was insufficiently observed, so we could only constraint a long period with $TP > 10$ h not possible to check against any other result. Also 410195 was insufficiently observed and is a slow rotator for which we could only give a lower limit $TP > 10$ h. Its published period is $P = 48.05$ h U $= 2$ (according to ALCDEF). 423747 was observed during 3 nights and shows a very small amplitude. Its tentative fit gives $TP = 4.14 \pm 0.01$ h but this should be regarded with prudence. It has no other published data. 425713 was observed during two nights and its data is quite scattered. We could fit a tentative period to $TP = 3.499 \pm 0.002$ h (with another solution $TP = 6.21$ h possible) which compares with the published value $P = 6.010$ h U $= 2+$ from the ALCDEF database. 2014 QK434 was observed during 3 nights but seems to have a very long period which will be discussed later.

The two LS-Dan runs produced the following tentative results for all 5 observed targets (Appendix Fig. 15). 39796, 399307 and 408980 will be discussed later. 86326 was observed during two nights and has a small amplitude. Our tentative fit $TP = 4.98 \pm 0.03$ h and its spectrum does not match the published period $P = 6.36$ h or its half dual derived by Warner (2015f). We observed 2014 SS1 during 2 nights for 6 h in total, which suggested a slow rotator with $TP > 10$ h. Again, B. Warner solved this object in the same time, establishing its period $P = 16.63$ h (Warner 2015i).

We derived tentative periods for the following 9 targets observed with ORM-INT (Appendix Fig. 16): 24443 shows few possible solutions above 4 h in its spectrum, and our tentative fit $TP = 5.8048 \pm 0.0001$ h should be regarded with caution due to the short overlap. Two ALCDEF listed values of B. Warner are $P = 4.069$ h and $P = 4.904$ h U $= 2$. 162980 was observed in alternance and only one night, impossible to derive any period, but its raw plot suggests slow rotation $TP > 10$ h. B. Warner observed it during 8 nights during the same time, suggesting $P = 12.71$ h U $= 2$ (Warner 2015j). 337866 was observed during half night but it was incompletely covered. Despite the small amplitude, it shows lots of details. We could only give a lower limit $TP > 7$ h which does not confirm $P = 5.1$ h reported by Carbognani and Buzzi (2016) but could confirm the solution $P = 8.955$ h of Warner (2016c). 377732 and 391033 will be discussed later. 410088 was marginally uncovered and could be tentatively fit with $TP = 2.377 \pm 0.003$ h which possibly represents the dual half published value $P = 4.781$ h U $= 2+$ (Warner 2015a) and shows other possible candidates in its spectrum. 416151 was observed for only 4 h which probably covered at least half spin, so we can only tentatively assume $TP > 8$ h which agrees with its published period $P = 12.191$ h after 5 nights by Warner (2015a). 427684 was observed to descend for 3 h, resulting in a lower constrain $TP > 6$ h, within the adopted period $P = 8.962$ h by Warner (2015a). 429584 will be discussed later. 2013 AV60 was undersampled and observed in full Moon conditions, and it has no published data. We can suggest a tentative period around $TP = 3.25 \pm 0.59$ h. Period fits for other three ORM-INT targets could not be attempted: 411280 (2010 SL13) was observed only half night and shows extremely small amplitude, impossible to solve. Its adopted period is $P = 7.79$ h U $= 2$ by Warner (2014d). 415986 was observed for only 1 h before

clouds cut the night, and it shows very large scatter. It has no published data. 429584 will be discussed later.

Buc-T50 derived tentative periods for 2 targets (Appendix Fig. 12), both having small amplitudes, difficult to solve using small aperture, small field and poor site. 285944 was observed during 4 nights in many fields whose zero points and possible offsets are quite sensitive to the comparison stars catalogues, and we tentatively give $TP = 2.35 \pm 0.01$ h which comes close to the adopted $P = 2.2455$ h by Elenin et al. (2015). 363814 was another very low amplitude target studied for the first time, tentatively solved in $TP = 6.6 \pm 0.1$ h, which should be regarded with prudence.

Despite its largest apperture, ORM-WHT could only poorly resolve 101955 Bennu $P = 4.10$ h (Appendix Fig. 17), which will be discussed later.

## 4.4 Known Binary Candidates

The study of binary asteroids is important in order to constrain the formation, evolution and physical properties of minor planets, and in particular NEA approaches represent great research opportunity for small telescopes. A first historic review about binary asteroid searches was published by Merline et al. (2002), followed by another one by Pravec et al. (2007). Four observing methods have been used to discover binary asteroids, namely:

- Stellar occultations, which need very precise astrometry and many observers, featuring the first binary asteroid Herculina ever discovered in 1978 by E. Bowell via photoelectric observations (Bowell et al. 1978);
- Direct imaging, which needs large telescopes and very good seeing, such as CFHT which discovered Eugenia's moon using near infrared and adaptive optics (Merline et al. 1999) and the Galileo mission which discovered Ida's satellite;
- Radar observations, feasible only for NEAs and PHAs coming closer to Earth and performed only by two USA antennas (Arecibo and Goldstone) which are leading the count with 43 discoveries[11];
- Lightcurve observations, feasible at both larger distances for MBAs and closer for NEAs, and available to smaller telescopes.

The first author who studied "anomalous" asteroid lightcurves was Cellino et al. (1985), followed by Pravec and Hahn (1997); Pravec et al. (1998b) who has continued to scrutinize this field much deeper (Pravec et al. 2006; Pravec and Harris 2007; Pravec et al. 2002, 2012, 2014, 2016). About 15% of all NEAs evolve into co-orbiting binary asteroids with well-separated components, according to Bottke and Melosh (1996) who modeled close encounters of fast-rotating contact-binaries and who counted doublet craters on Earth and Venus. This result was confirmed first by Margot et al. (2002) who counted results of a radar survey of 50 NEAs and evidenced about 16% to be binary, then by Pravec who found at least 15% suspected binaries from the known NEA population larger than 300 m (Pravec et al. 2006).

By March 2017 there are 266 confirmed and 72 suspected binary asteroids, according to LCDB database. Checking our targets, there are 4 known binaries (5143, 163693 Atira, 348400 and 399307) and 3 other possible binaries (2102, 3352 and 68348), two of them discovered by B. Warner based on data taken independently in the same period with our observations. We discuss next these 7 binary systems.

---

[11] https://echo.jpl.nasa.gov/~lance/binary.neas.html.

To derive binary periods we used the "Dual Period Search" tool in Canopus, which is based on a iterative substraction process proposed first by Pravec et al. (2006). First, the approximate primary period (P1) is derived from the composed lightcurve, which is subtracted from the curve, leading to a first approximate secondary period (P2). Second, the secondary contribution P2 is subtracted from the original curve, which allows finding a refined primary P1. By continuing a few steps this procedure (upon saving at each step all Fourier parameters), one can satisafactory fit both P1 and P2.

PHA 2102 Tantalus was observed first by P. Pravec et al. in 1994/95 who derived a weighted average period $P = 2.391$ h U $= 2$ but did not suspect any binarity (Pravec et al. 1997). Based on 5 nights observations in 2014, Warner (2015k) concluded that Tantalus is a probable binary and derived $P1 = 2.384$ h the period of the primary (U $= 2+$) plus a strong secondary solution $P2 = 16.49$ h of the supposed satellite, although he did not see any mutual events. Using his private IAO-T35 telescope during 5 nights in 2017, A. Aznar could solve both the primary $P1 = 2.3865$ h and secondary period $P2 = 8.2177$ h (fits in Fig. 2) which represents half of P2 derived by Warner and should be regarded with caution, especially for being derived in very difficult amplitude conditions.

3352 McAuliffe was observed first by P. Pravec in 1998 who tentatively derived $P = 6$ h U $= 1$. In 2012, J. A. Howell observed McAuliffe during 5 nights and derived $P = 2.207$ h U $= 2+$ with no binarity suspected (Howell 2012). Based on 2012 observations during 7 nights, Warner (2012) conducted a dual period analysis and derived $P1 = 2.2060$ h and $P2 = 20.86$ h in very low amplitude and insecure conditions (other solutions being possible). During 3 nights in 25-27 Sep 2016, B. Warner re-observed McAuliffe and derived $P = 2.212$ h with no signs of binarity (Warner 2017c). Using the IAO-T35 telescope during 4 nights in late Nov 2016, A. Aznar derived $P = 4.504$ h with other few minima visible on the phase spectrum (Fig. 2) and one peak less probable at previously known half dual solution. No signs of binarity were detected and the restrained data prevented a dual analyse.

The large NEA 5143 Heracles (4.5 km) is a known Q-type asteroid previously studied by us spectroscopically, part of the Taurid Complex (Popescu et al. 2014). Its photometric observations were acquired since 1998 by many authors, and its adopted ALCDEF period is $P = 2.7063$ h U $= 3$ by F. Pilcher et al., based on 2011 coordinated observations (Pilcher 2012). Based on this data, P. Pravec found strong but insufficient evidence of binarity (3 dips characteristic for transits, occultations or shadow events), but could not derive the revolution of any possible satellite. In Dec 2011 the Arecibo radar discovered a satellite of Heracles. Since then, there was no confirmation of the binarity based on lightcurve observations. In 2016 A. Aznar used his private IAO-T35 telescope to observe Heracles during 12 nights (8–18 Nov 2016 and 14–17 Sep 2016), taking in total 774 images. Joining this data with observations made by Daniel Bamberger and Guy Wells (Northolt Branch Observatories, UK), B. Warner (Palmer Divide Observatory, USA) and R. Naves (Montcabrer Observatory, Spain), Aznar could resolve a dual period of Heracles: $P1 = 2.7086$ h and $P2 = 17.114$ h which matches the result of a recent Arecibo radar detection (P. Taylor—private communication). We include the two fits in Fig. 2. Based on our findings, we derive a ratio between the sizes of the two bodies $D2/D1 \geq 0.23 \pm 17\%$ (assuming the same albedo for the two bodies), which matches within errors previous results $D2/D1 \geq 0.17 \pm 50\%$), thus the size of the satellite is $850 \pm 150$ m revolving every 17 h around the primary (Aznar Macias 2017).

68348 was observed first by B. Skiff in 2011 who derived $P = 3.324$ h U $= 3-$ (the ALCDEF adopted value) but did not report any indication of a satellite (Skiff 2011; Warner 2015k). Based on 2015 data taken independently and simultaneously with our

observations, B. Warner was the first who suggested binarity with a primary period $P1 = 3.8759$ h $U = 2+$ and a satellite with secondary period $P = 17.54$ h (Warner 2015k). Using the Mod-T60 data, Galád found the primary period $P1 = 3.3313$ h and could fit a secondary period $P2 = 9.20$ h (plots included in Fig. 5) which is about half the result of B. Warner.

163693 Atira is a large binary system (about 2 km primary) moving in an interior Earth orbit (IEO). In 2003 P. Pravec resolved its rotation to $P = 3.3984$ h $U = 2$ and recently one moon was discovered by radar by Rivera-Valentin et al. (2017). Using the OSN-T90 telescope during 4 nights, we recently resolved its period $P = 3.3980$ h (Fig. 7) but could not detect any sign of binarity.

348400 was observed during 3 nights with Buc-T50 (Fig. 3). The fit of more nights was risky due to the very low amplitude and lack of details, so we attempted to fit each night independently. The second night provided best data which resulted in a candidate period $P = 2.43$ h (presented next in Fig. 3 and adopted by us), followed by the third night which gave $P = 2.30$ h. Both these findings are close to the adopted $P = 2.4149$ h observed during 5 months by J. Oey (U = 3) who published many fits and evidenced the existence of a satellite (Oey and Groom 2016) later confirmed by radar.

399307 was observed with LS-Dan during 3 consecutive nights for 5 h (in alternance with other objects) and had no known binarity status before. Each night shows similar "V"-like patterns, slightly different in amplitude and width (see Fig. 15) which later suggested the possibility of a binary object. Unfortunately, the sparse data and limited number of nights prevents any detailed analysis, and a tentative fit based on available poor data gives $TP = 7$ h. Based on many observations taken in the same time during 15 nights using 4 small telescopes located in USA, Chile and Australia, B. Warner et al. discovered $P1 = 3.4907$ h for the primary object and a satellite with orbital period $P2 = 15.917$ h (Warner 2015g).

### 4.5 Known Tumbling Candidates

In 1994 A. Harris presented a first paper dedicated to non-principal axis rotators (NPA rotators), known also as "tumbling asteroids" (Harris 1994). In 1995 Hudson and Ostro identified by radar the first tumbling asteroid, (4179) Toutatis, which rotates in a long-axis mode characterized by periods of 5.41 days (rotation about the long axis) and 7.35 days (average for long-axis precession) (Hudson and Ostro 1995; Spencer et al. 1995). Other tumbling objects were studied by Mottola et al. (1995), Pravec et al. (1998a) (based on lightcurve observations) and Benner et al. (2002) (based on radar data). More recently, the tumbling state of another famous NEA, namely Apophis, was studied (Pravec et al. 2014). In 2001 Kaasalainen showed that the lightcurves of freely precessing asteroids can be analysed using the same methods as with single periodic objects (in relaxed rotation) and presented an inversion procedure with examples (Kaasalainen 2001). The use of two-dimensional Fourier series (angles $\psi$ and $\phi$) which describes a tumbling lightcurve differs from the simple sum of two independent Fourier series used for binaries, but Canopus is not endowed yet with any NPA model. In 2005 P. Pravec reviewed this topic, defining the *PAR* codes aimed to distinguish NPA objects from regular PA (principal axis rotators), and presenting old and new tumbling asteroids (Pravec et al. 2005). He suggested that most asteroids larger than $\sim 0.4$ km with estimated damping timescales equal or larger than the age of the Solar System are NPA rotators.

By March 2017 there are 74 known NEA tumblers in the LCDB database, denoted with "T+" (confirmed) or "T?" (suspected). Most of them show periods of a few dozen hours

and there is not clear if a lower limit exist. In our survey we evidenced a few relatively large and very slow NEAs apparently showing fast rotation secondary periods, possibly associated with tumbling state or satellite systems. Checking the ALCDEF database (at 5 Mar 2017) for all objects observed in our survey, we found 8 possible objects: 4 marked with flag "T?" in the Notes[12] (possible tumblers showing some observational evidence), plus other 4 objects marked with code "T0" (possible tumblers but need more observations to decide). We will discuss next these objects, and suggest other few unknown tumbling candidates.

9400 is a very large Amor NEA (3.5 km) and known very slow rotator. It was observed with Buc-T50 in Sep–Oct 2015 (Fig. 3) and resulted in a candidate fit $P = 82.6$ h which is relatively close to the published $P = 97.1$ h U $= 2$ value of Warner (2016d) and coincides with his earlier result (observed in the same period with us) $P = 82.8$ h U $= 2$ (Warner 2016e). From both publications, B. Warner concluded that 9400 is probably tumbling, given the slopes of the individual nights which do not follow the slope of the Fourier model curves (for his 2015 data) and the high steepness of the slopes (for his 2016 data). We observed it in Sep–Oct 2015 using the Buc-T50 telescope and we confirm that two sessions have opposite tilt from our main Fourier fit $P = 82.6$ h.

388945 was observed during 2 nights (total only 3 h) by MOD-T60 and its by far incomplete lightcurve resulted in a tentative period $TP = 7.5$ h (Appendix Fig. 13) which must be regarded more as a lower limit, due to the very small coverage. This does not match any of the best single period fits $P1 = 44.2$ h and $P2 = 52.4$ h U $= 2$ of B. Warner which "do not necessarily represent a solution for rotation and precession" but suggest a tumbling state (Warner 2016g).

2014 CU13 was observed during 2 nights by MOD-T60 and its tentative period $TP = 7.18$ h (Appendix Fig. 13). This matches half the published period $P = 14.36$ h U $= 2$ selected from 3 possible solutions of Warner (2014c) who suggested tumbling state in some conditions (PAR=-1 in ALCDEF). Clearly, our MOD-T60 plot shows unusual spread of the points across the direction of the fitted curve and it seems to follow small paths in at least few places.

39796 was observed for 8 h during the first night of our second Danish run, in alternance with another object. Preliminary data reduction suggests a very slow rotator which we decided to drop given the limited time (only two nights available). Based on this poor data (presented in the Appendix Fig. 15), we derived a lower limit $TP > 10$ h. Indeed, this is an extremely slow rotator with published period $P = 223.5$ h by Warner (2015e). Based on the slopes of individual sessions which do not follow the slope of the Fourier model curve and the expected dumping time for tumbling which exceeds the age of the Solar System, B. Warner found this slow rotator likely tumbling (Warner 2015e).

470510 (2008 CJ116) is a relatively large NEA (between half and one km). It was observed by us with the IAO-T35 telescope during 9 nights (Fig. 2). Its lightcurve could be solved with the 3 order long period $P = 32.644$ h which matches the result of B. Warner $P = 32.36$ h who suggested this object is possibly in a tumbling state but did not find any evidence (Warner 2017d).

2014 QK434 is a tumbling candidate, based on its large size (half to one km) and very slow rotation determined from 7 night observations in 2015 by B. Warner who fits a very slow solution $P = 78.4$ h but could not find on his plots any tumbling evidence (Warner 2015d). We observed it insufficiently with ORM-Mer, so any fit guess is risky (Appendix Fig. 14). Its raw plot shows some oscillations and big jumps which suggest a long period.

---

[12] http://www.minorplanet.info/datazips/LCDB_readme.txt.

242708 is a big Apollo NEA (max 1.6 km). Its ALCDEF period is $P = 4.289$ h based on a very noisy fit U = 1+ of (Carbognani 2014). We observed it during 7 nights with MOD-T60 and it seems to be a very slow rotator tentatively fit by $TP1 = 63.8$ h, but incompletely sampled (Appendix Fig. 13). Every session shows a tilt different than that of the main fit, and at least two nights show a clear zigzag pattern, suggesting a secondary period for this tumbling candidate.

2009 DO111 is a fast rotator (about 3 min) which became a great opportunity in 2009 for a newly discovered smaller NEA (82–185 m acc to the NEODyS database[13]) to be accessible in good conditions ($V = 15.4$) by smaller telescopes, which included MOD-T60. It was observed and published online first in 2009 by R. Behrend[14] who found $P = 0.0020374$ h (recorded in ALCDEF as $P = 0.04890$ h) and mentioned "Provisoire. Objet virevoltant (=tumbler)! A reanalyser finement", thus suspecting a tumbling state (although it is not marked accordingly in the Notes in ALCDEF). In 2014 the period was derived by B. W. Koehn (NEAPS program at Lowell Observatory) who found $P = 0.04887$ h and suggested also possible the dual double period after "significant shifts in magnitude" for sub-sessions were needed to be able to fit (Koehn et al. 2009) (ALCDEF recording it as quite uncertain, U = 1+). We used MOD-T60 to observe 2009 DO111 during the night of 16 Mar 2009, and we believe we could improve now previous results to $P = 0.0488781$ h (Fig. 5). Nevertheless, our coverage is insufficient to test the tumbling supposition.

## 4.6 New Tumbling or Binary Candidates

We observed rapid oscillations (few minutes) for 8 relatively large NEAs, including 2 previously suspected tumbling systems, other 5 unknown objects possible tumbling or binary systems and probably one binary NEA. We will discuss these objects here.

391033 is a large Amor NEA (half to one km) which was observed extensively (one month) by Warner in 2014 who derived a very long period $P = 850 \pm 100$ h U = 2 and suspected this object as a good tumbling candidate, although he did not see obvious signs in the slopes of the individual sessions (Warner 2015l). The ORM-INT data taken during 2 nights (in alternance during first night and only 6h total) shows a slow grow consistent with a very slow rotator (Appendix Fig. 16) and some clear zigzag patterns along the main growing trend which could be fit tentatively each night with a very fast order 3 solution $TP2 \sim 0.1400 \pm 0.0001$ h. The same solution was found fitting first night ($TP2 = 0.1413$ h), second night ($TP2 = 0.1483$ h) and both nights ($TP2 = 0.1400$ h) after arbitrarily offset by +0.075 mag of the second night to accommodate for the main grow. In the Appendix Fig. 16 we include the Fourier fit of the first night (spanning longer time), both nights, and the period spectra of both nights. The short period $P2$ could be either the second period of the possible tumbling state or the evidence of a fast spinning satellite of this NEA.

429584 (2011 EU29) is a relatively large (around half km) NEA suspected tumbling candidate by B. Warner who covered it during 8 nights and found a long period $P = 43.5$ h but no signs of tumbling on his plots (Warner 2015p). We observed this object with the ORM-INT as a follow-up of another longer campaign from Tenerife using the ESA-OGS 1m and IAC80 telescopes which alerted the ORM-INT to check for rapid spin. Using the ORM-INT we observed this object in bright conditions during 2 nights, apparently

---

[13] http://newton.dm.unipi.it/neodys.

[14] https://obswww.unige.ch/~behrend/page5cou.html#09db1o.

sampling some maximum during first night (within 0.03 mag), then a clear descend during second night (leveling to the end) whose tilt does not align well with the first night (Appendix Fig. 16). Although small oscillations seem visible during both nights, any fast solution is risky due to the very small amplitude and larger uncertainties caused by the bright Moon. We will follow up this object in our next paper which will join our 3 telescope datasets (Cornea et al. 2017).

27346 is a large Amor NEA (1.753 km) with no published lightcurve. We observed it insufficiently with ORM-Mer during only one night (2 h), before clouds spoiled the rest of the run. Its curve is quite flat within $\sim 0.1$ mag (Appendix Fig. 14) suggesting a spherical object, pole sight-on direction or very slow rotation. Apparently, a very short period could be tentatively fit independently in $r$ ($TP2 = 0.069 \pm 0.001$ h), in $g$ ($TP2 = 0.068 \pm 0.001$ h) and also in the $g - r$ color plot—to be discussed later ($TP2 = 0.072 \pm 0.001$ h) which could be associated with the spin of a satellite or eventually with the short period of a tumbling state. Observing that this period is very close to 4 min (meaning twice our effective cadence), we should regard this tentative result with prudence.

112985 is a large (2–5 km) Amor NEA listed with $P = 4.787$ h U = 2 in the ALCDEF based on 10 nights in Nov 2015 observed by Warner (2016f), but having other two different possible solutions derived by the same author based on other available data sets: $P = 5.94$ h U = 2 based on 6 nights in Apr 2015 (Warner 2015m) and $P = 3.820$ h U = 2 based on 4 nights in Jul 2015 (Warner 2015e). A fourth different result was found by A. Carbognani with $P = 3.436$ h U = 2− based on 5 h data taken during one night in Apr 2015. Clearly, this object or system remains very ambiguous. We observed 112985 with ORM-Mer during only one night (2 h) and have attempted another night when the clouds prevented any good data. Nevertheless, using the one night data we could evidence a fast solution. In the Appendix Fig. 14 we include the ORM-Mer $r$ and $g$ raw plots ($r$ above and $g$ bellow) which show some oscillations (especially in $g$ band which has larger amplitude). The $r$ fit and period spectrum come next, followed by the $g$ fit and its period spectrum. The uncertainties are quite large because of the faintness of the object ($V = 19.2$), its low altitude and gray Moon $35°$ nearby. The tentative fit of 112985 in $r$ gives $TP2 = 0.151 \pm 0.02$ h and the fit in $g$ gives $TP2 = 0.353 \pm 0.006$ h which matches the $g - r$ color fit (to be discussed later), adopted by us as the second period for this object or system. More than one month later, we re-observed 112985 part of the Tenerife survey using the IAC80 telescope, and some rapid oscillations were indeed visible in the LiDAS plot, to be presented in our next paper (Cornea et al. 2017).

285625 is another large Amor NEA (1–2 km) not published before. We observed it during 2 nights (7 h total) with ORM-Mer and we could evidence a fast solution possibly related to tumbling or a satellite. The raw plots look quite flat but show some clear variations especially in $g$ band (Appendix Fig. 14) and we plot both nights (with $r$ band above and $g$ bellow). Apparently few fast solutions could be fit, and in particular we include first night in $r$, second night in $g$ and both nights in $g$, which all tentatively conclude to $TP2 = 0.066 \pm 0.001$ h, which agrees with the color plot (to be discussed later). This object was followed two nights later from Tenerife using the OGS 1m telescope, which apparently proved the oscillation; we will present the combined data in our next paper (Cornea et al. 2017).

377732 is a large (1 km) Apollo NEA having no published period. We observed it with the ORM-INT during only 2 h and its curve looks quite flat (Appendix Fig. 16), slowly descending, suggesting a very slow rotator. Some unusual oscillations could be seen which can be fit quite well with a 4 order tentative solution $TP2 = 0.132 \pm 0.001$ h in small

amplitude conditions, moreover other solutions could be seen, so this result should be regarded with prudence.

408980 (2002 RB126) was observed during 3 nights with LS-Dan in alternance with another object. It shows unusual scattered data along the $Y$ axis compared with uncertainties (see the raw nightly plots in the Appendix Fig. 15) and a small amplitude which generates few tentative fits $TP$ between 2–10 h. Using data taken 2 weeks before us during 4 nights, B. Warner established $P = 16.21$ h with dual half period also possible (Warner 2015h). Observing that this is a large object (up to 1.3 km) and taking into account the relatively long period and our unusual scatter along Y, we could suggest a very short period possibly caused by either a small satellite or tumbling state.

2011 WO41 is a large (1.5–3 km) Apollo NEA listed in ALCDEF with $P = 4.609$ h (U = 2 ambiguous result). We observed it during 8 nights using the IAO-T35 telescope (total 29 h) and it shows a low amplitude. The usual fit attempt (presented first in Fig. 2) provided $P = 13.33$ h and showed a few unusual drops in a few sessions (especially one at 0.9 in phase curve), probably suggesting a binary system. Considering the two period analyse in Canopus, A. Aznar derived $P1 = 5.73$ h the rotation period of the main body (adopted as our candidate result) and $P2 = 17.66$ h for the synodic period of the assumed satellite (both fits following in Fig. 2). Considering a 0.10 mag drop due to a mutual event with the satellite (corresponding to phase 0.9 in the first plot) and assuming 0.21 mag maximum amplitude of the lightcurve, then the system size ratio should be around $D2/D1 = 0.3$.

## 4.7 Special Targets

We present next 4 special objects whose apparition triggered dedicated runs using 2 largest available telescopes (ORM-INT and ORM-WHT) and/or participation in international campaigns.

### 4.7.1 Possible "Deep Impact" Extended Mission (163249) 2002 GT

During the IPEWG workshop in Nice (May 2013), Steven Chesley (NASA/JPL) pointed the need of an international campaign to observe the potential hazardous asteroid (PHA) 2002 GT, possible target of the extended *Deep Impact* Mission, unfortunately canceled in September 2013.[15] Four telescopes joined this campaign: 0.65 m in Ondřejov (Czech Republic), 0.77 m in La Hita and 1.2 m Calar Alto (Spain) and the TMO 1 m telescope in Table Mountain Observatory (USA). During 3 h on 3/4 Jun 2013 we used the ORM-INT to follow this target. Our dataset covered a bit less than the actual period (Fig. 10), but could be well fit with a period $P = 3.94$ h (with $\sigma = 0.003$ mag in the individual asteroid measurements), which is very close to the ALCDEF adopted value ($P = 3.7663$ h).

All data was analised by Petr Pravec who led this campaign and pointed out that data from two telescopes (ORM-INT and TMO) showed a shift towards the end part of the curve with respect with denser data collected by other 3 telescopes located in continental Europe. Three reducers (Jana Chesley in USA, V. Tudor and O. Vaduvescu in La Palma) used different software to reduce independently the ORM-INT data, taking extra care with flat field correction and comparison stars. In the end, some small offsets still stand (although the differences were reduced) which could not be explained. Observing that the ORM-INT and TMO are the Southernmost stations participating in this campaign, one

---

could possibly speculate some evidence of a mutual event with a satellite otherwise not seen by the other three Northern stations.

### 4.7.2 The Very Fast Rotator 2014 NL52 discovered by EURONEAR

Part of the ORM-INT NEA 2014-2016 recovery campaign of one opposition NEAs (PI: O. Vaduvescu), during the night of 10/11 Jul 2014 the IAC service observer Olga Zamora serendipitously imaged one field in which the reducer Lucian Hudin (amateur astronomer, Romania) promptly flagged one trailing object ($\mu = 6''/min$) as a NEA candidate. Following its recovery by other stations, this asteroid became the second secured EURO-NEAR NEA discovery, a relatively small Apollo object with size between 57 and 128 m (Vaduvescu 2015).

Interestingly, in the six blinked discovery images Lucian Hudin visually noticed variation in the asteroid brightness (sometimes along the trails) and alerted the PI for possible follow-up regarding the possibility of very fast spin. Advised by the EURONEAR member Tomasz Kwiatkowski, O. Vaduvescu used two telescopes in La Palma (Liverpool LT 2 m and the ORM-INT) in fast cadence (25 s exposures in a small $5 \times 5$ arcmin window), and the noisy but multiple coverage (during 2 h) INT data resulted indeed in very fast spin $P = 4.459 \pm 0.003$ min. Later independent reduction by O. Vaduvescu in Canopus of the same data confirmed $P = 0.0743$ h, followed by other two solutions with larger RMS (see the period spectrum in Fig. 10).

### 4.7.3 The "Halloween Asteroid" 2015 TB145

Discovered by Pan-STARRS 1 survey at 10 October 2015, this Apollo PHA roughly 600 m in diameter and absolute magnitude $H = 20$ is possibly a dead comet which safely passed Earth at 1.3 lunar distance on 31 October 2015. Promptly, the media has nicknamed it the "Halloween Asteroid", the "Great Pumpkin" and the "Skull Asteroid" due to its human skull-like appearance following radar images taken by Arecibo Observatory [16] which suggested its rotation period of about 5 h.

We observed 2015 TB145 during flyby with four telescopes: ORM-INT (3h during 27/28 Oct 2015), OT-IAC80 (5h during 28/29 Oct night and other 5h during 29/30 Oct), IAO-T35 (4h during 29/30 Oct) and Buc-T50 (total of 11h during 28/29, 29/30 and 30/31 Oct nights). The conditions were very difficult due to increasing apparent motion (from 1 to more than $10''/min$) and close proximity of full Moon (located from 40 to 15 degrees from the target) and we could not include the two small telescopes in the fit.

The ORM-INT 3h dataset resulted the best ($0.004 < \sigma < 0.008$ mag in final asteroid measurements), but it was insufficient to cover one complete rotation. We include a possible fit (Fig. 6) which should be regarded as a tentative minimum limit, $TP > 3.9 \pm 0.2$ h. The OT-IAC80 covered $5 + 5$h during two nights but was noisier (especially during second night when the exposures were shorter). This dataset had to be processed very carefully due to the proximity of the Moon which induced high and rapidly changing sky gradient which needed to be built from a few groups composed by the science images, then subtracted from each field. We present second in Fig. 6 the phase fit obtained from the ORM-INT and the IAC80 first night data (freely adjusted to the absolute ORM-INT dataset) resulting in a tentative long period $TP = 7.47$ h which should be regarded with caution. Finally, we present our resolved period considering both OT-IAC80

---

[16] http://www.jpl.nasa.gov/news/news.php?feature=4760.

nights plus the ORM-INT data, fitted with the phase dispersion minimization method (Stellingwerf 1978): $P = 4.80 \pm 0.07$ h.

Our main solution agrees well with the second possible solution of Muller et al. (2017) who used the VLT-VISIR in mid-infrared and visible observations with the Calar Alto 1.2 m, Sierra Nevada 1.5 m and La Hita 0.8 m telescopes in Spain, linking results with data from J. Oey (Australia) and B. Warner (USA), which covered together 10 nights (21-31 Oct 2015), to derive $P = 4.779$ h. Their preferred period $P = 2.939$ h is affected by large scatter, actually being very close in $\chi^2$ to their second period, and it remains well bellow our best ORM-INT limit.

### 4.7.4 The OSIRIS-REx Target (101955) Bennu

The Virtual Impactor (VI) asteroid Bennu (101955) = 1999 RQ36 is an Apollo PHA discovered by the LINEAR survey at 11 Sep 1999. According to the NEODyS database, it has a diameter of half kilometer and a remote chance to impact Earth (less than 0.04%) between 2175 and 2199. It was set as the target of the OSIRIS-REx NASA mission [17] to study a primitive asteroid and return a sample to Earth in 2023.

During 2011 we observed Bennu during 3 service nights relatively spaced in time: 29/30 Aug, 13/14 Sep and 4/5 Nov 2011. We planned relatively short observing sessions, being forced by the difficult conditions during this apparition: small Solar elongation (106°, 86° and 96°, respectively), faint magnitude ($V = 19.9$, 20.2 and 21.8 mag, respectively), fast proper motion ($\mu = 5.1$ ″/min during second night) and the Moon (full during second and third night). The first two runs were affected by cirus, while the third was photometric but the target was fainter.

Our first approach to reduce the data using aperture phomometry in IRAF `phot` package resulted in relatively large uncertainties ($\sigma \sim 0.1$ mag) owing to the full Moon and fast proper motion which forced us to use short exposures (20 s). In 2013 we engaged first in reducing the data using PSF photometry in IRAF `daophot` package, and the first results were encouraging, although no reduction package was available and the manual work was tedious. In 2015 Vlad Tudor implemented PSF photometry in LiDAS, which was recently used to measure Bennu's PSF photometry 3-4 times more accurate than using aperture photometry (PSF typical $\sigma \sim 0.04$ mag for first two nights).

We present in the Appendix (Fig. 17) first the raw nightly plots (n1, n2 and n3), based on LiDAS PSF photometry (above, in red squares) and aperture photometry (below, in dark triangles) shown for n3 for comparison. Fourier fits of order 2 and 4 follow next, joining n2 and n3 data only, while n1 data could not be fitted due to changes in phase angle during more than two months interval of our service observations. We provide two tentative results, fitted with order 2 ($TP = 2.19 \pm 0.01$ h) and order 4 ($TP = 4.10 \pm 0.01$ h). Previous periods published $P = 2.146$ h based on 1999 data (Krugly et al. 2002), $P = 4.2968$ h (Hergenrother et al. 2012) adopted by ALCDEF), $P = 4.29746$ h (Nolan et al. 2013), and $P = 4.2905$, h (Hergenrother et al. 2013) all based on 2005 observations. Apparently, no rotation period was determined during the 2011 apparition, due to the difficult observing conditions. Due to the non-photometric conditions during first two runs and lack of accurate fainter catalog stars in these sessions (which do not saturate in the ORM-WHT images), we could not secure any color indices for Bennu.

---

[17] https://www.nasa.gov/osiris-rex.

# 5 Mercator Color Lightcurves and Indices

Very few authors attempted color variation along the rotation of the asteroids and probably nobody has attempted before simultaneous multi-band imaging. This technique could be used to derive information about changes in morphology, albedo changes across the surface or eventually binarity otherwise not detectable from one-band lightcurves. We review first some previous results.

In 2002 Sekiguchi et al. made the first attempt to address the color change over rotation of a Solar system body (Sekiguchi et al. 2002), namely the trans-Neptunian object 1996 TO66 whose rotation period $P = 6.25$ h was known before. Choosing the Bessel $V$ and $R$ filters of the FORS1 camera mounted on the UT1 ESO-VLT telescope, the authors used relatively sparse (2–3 consecutive and binned) images to evidence color changes along the rotation phase with a maximum amplitude $V - R = 0.10$ mag and affected by larger errors in the first part. In 2004 F. Yoshida published photometry and colors of the MBA (832) Karin, the largest body of the very young Karin family (Yoshida et al. 2004). She alternated the *BVRI* filters mounted on the 1.8 m Vatican telescope (VATT, USA) finding a rotation period $P = 18.35$ h and little color variation (mostly in the $V - I$) along their sparsely sampled phase curve (only 6 points obtained by interpolation for all filters to the same moments). In 2007 D. Kinoshita and colleagues studied the lightcurve and color indices of the Apollo NEA 155140 (2005 UD, 1.3 km diam) supposed to be a fragment of the larger NEA (3200) Phaeton (Kinoshita et al. 2007). Using the 1 m telescope at Lulin observatory in Taiwan, the authors took series of images in alternating *BVRI* filters, deriving some variation in the color plots (especially in the $R - I$) but which are inconsistent with previous findings.

Given the great capability of the Mercator MAIA camera to acquire simultaneous three band *ugr* imaging, we reduced both $r$ and $g$ data independently (all targets remaining invisible or giving very small signal in the $u$ band) with the aim to compare our $g$ or $r$ periods and to study the $g - r$ color variation as a function of time and synodic rotation. Color curves of 10 of the 14 NEAs observed with the ORM-Mer telescope could be fitted, and for 5 of them we found periods matching or very close to the mono-color $r$ or/and $g$ fits. The other 4 NEAs showed scattered color fits, impossible or very risky to attempt any fitting. We present in Fig. 11 the color plots for the periods of 10 Mercator targets and in Table 3 we include measured $g - r$ color indices (given as minimum and maximum values), followed by the derived color rotation period and uncertainty (in hours). We underline in bold the color periods which match the adopted periods (found by us using one band or published by other authors). Color uncertainties are calculated as the square root of the sum or the squares of uncertainties in each band and plotted as error bars in Fig. 11. We will discuss next these color curves and fits.

The 12538 $g - r$ color lightcurve could be tentatively fitted with $TP = 3.77 \pm 0.02$ h and should be regarded with prudence. This comes between our adopted $P = 2.582$ h and its dual period $P = 5.154$ h preferred by B. Warner (ALCDEF database).

Despite larger uncertainties caused by cirrus, 27346 shows some oscillations which can be fit with a fast tentative $TP2 = 0.072$ mag. This comes very close to both our $r$ fit ($TP2 = 0.069$ h) and $g$ fit ($TP2 = 0.072$ h—see Appendix Fig. 13). These matches could not be mere coincidence, confirming our previous detection of a secondary period possibly associated with a small satellite (fast rotator $\sim 4$ min) whose surface shows visible changes detectable in its color lightcurve.
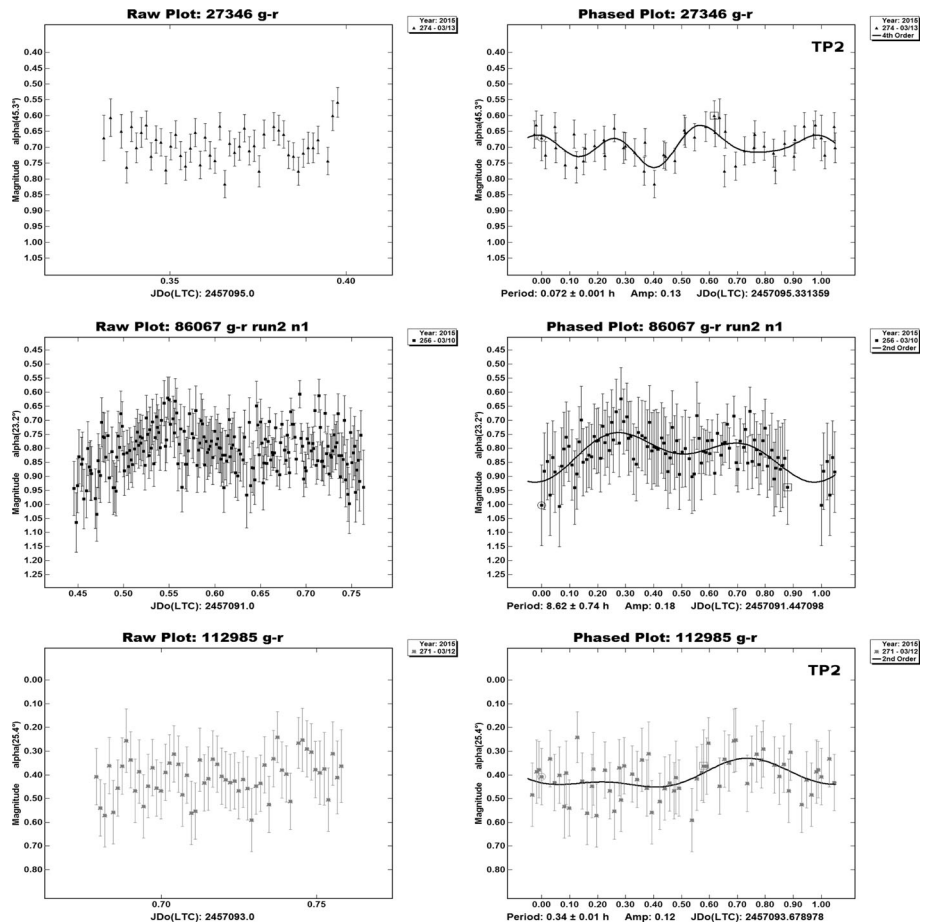
**Fig. 11** NEA color variation and $g - r$ color lightcurves observed with the Mercator telescope and MAIA camera

86067 follows clear changes in its raw color plot of first night of the second run which covers longest continuous time and was chosen for this study. The color plot could be fit with $P = 8.62$ h (marginally covered) which is close to both periods derived from our $r$ fit ($P = 9.1922$ h—adopted) and the $g$ fit ($P = 9.200$ h). Its published period is $P = 9.196$ $U = 3$—by Warner (2015n).

The raw color plot of 112985 suggests a sinusoidal-like trend which could be tentatively fit with $TP2 = 0.34$ h. This matches our adopted $g$ fit ($TP2 = 0.353$ h) and comes around the dual of our $r$ fit ($TP2 = 0.151$ h) which we did not prefer as possible rotation of a presumably satellite.

The $g - r$ color lightcurve of 175114 could be tentatively fitted with $TP = 9.70 \pm 0.4$ h which is quite close to the previous published value $P = 8.879$ h of B. Warner. This color fit should be regarded with caution, due to the very small (0.02 mag) and the incomplete sample.

Although incompletely covered, the color plot of 275976 could be tentatively fit with $TP = 6.41$ h which is the best solution in the color period spectrum. This comes very close
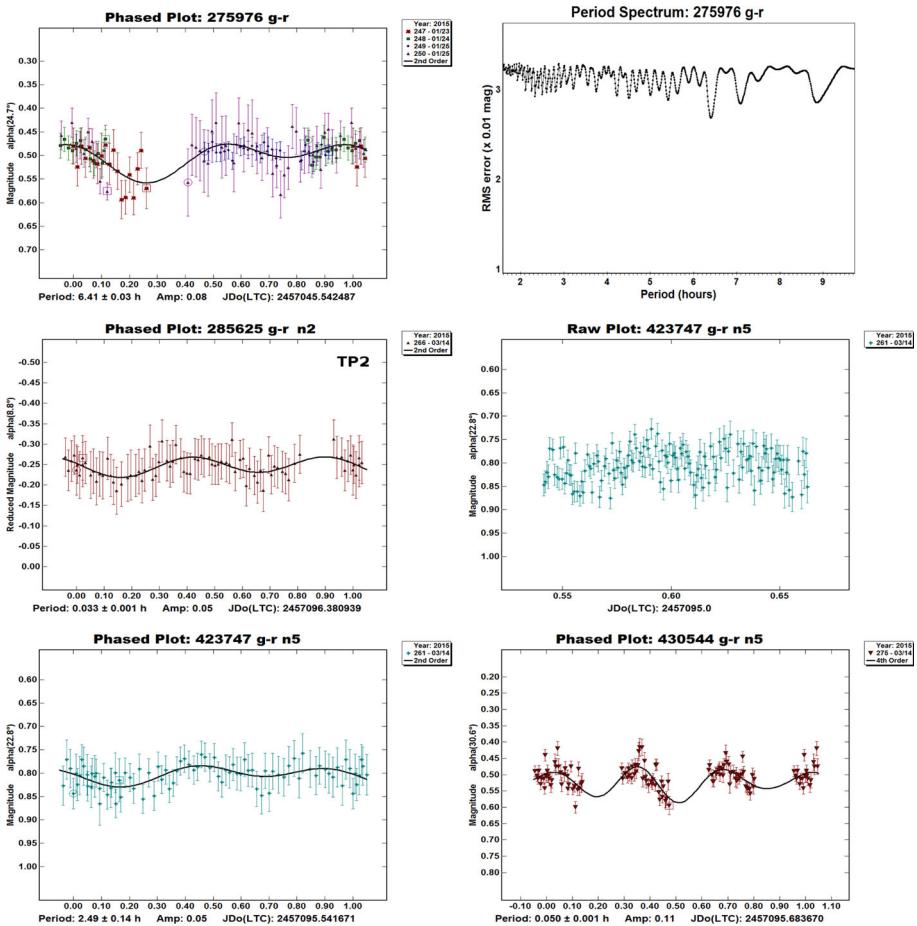
**Fig. 11** continued

to our adopted period $TP = 6.66$ h (in $r$ band) and quite close to the other longer solution in $g$.

The color plot of 285625 can be tentatively fit by a fast rotation $TP2 = 0.033$ h, which represents half dual of our preferred $g$ fit ($TP2 = 0.065$ h). It has no other published data.

The color of 410195 shows a clear sin-like variation along the raw plot, which could be tentatively fit by $TP = 3.25 \pm 0.4$ h, but this has extremely low amplitude (0.02 mag), thus it should be regarded with caution, moreover our tentative period was very long ($P > 10$ h), being based on its very slowly descending nightly curves.

Dropping some noise causing deviant points, the color plot of 423747 (one of the nights) shows clear changes which could be fit by $P = 2.49$ h, which is less than our candidate $P = 4.14$ h derived in the $r$ band.

Finally, 430544 shows a color plot which could be tentatively fit with a rapid solution $TP2 = 0.050$ h, which should be regarded with caution due to under-sampling and mismatch with the clearly adopted ALCDEF $P = 2.633$ h U = 3−.

**Table 3** The ORM-Mercator $g - r$ color indices and color fitted periods

| NEA | $g - r$ min | $g - r$ max | $P$ | $\sigma$ |
|---|---|---|---|---|
| 12538 | 0.65 | 0.75 | TP | – |
| 27346 | 0.60 | 0.75 | **0.072** | 1e-3 |
| 86067 | 0.75 | 0.95 | **8.6** | 7e-1 |
| 90416 | 0.32 | 0.38 | – | – |
| 112985 | 0.30 | 0.50 | **0.34** | 1e-2 |
| 175114 | 0.48 | 0.52 | TP | – |
| 275976 | 0.46 | 0.54 | **6.41** | 3e-2 |
| 285625 | 0.65 | 0.75 | 0.033 | 1e-3 |
| 322763 | 0.65 | 0.75 | – | – |
| 410195 | 0.55 | 0.57 | TP | – |
| 423747 | 0.75 | 0.85 | 2.5 | 1e-1 |
| 425713 | 0.60 | 0.75 | – | – |
| 430544 | 0.50 | 0.60 | 0.050 | 1e-3 |
| 2014 QK434 | 0.55 | 0.70 | – | – |

## 6 Conclusions

We resume here the main results of this survey:

- We present a lightcurve survey of 101 near Earth asteroids (NEAs) observed within the EURONEAR network between 2014 and 2017 (including few unpublished older objects) using 11 telescopes located in Spain, Chile, Slovakia and Romania. This is the second in a series of 4 papers.
- Most observed targets had no published data at the time of observing, nevertheless some objects were observed in the same period and were published in the meantime mainly by B. Warner (USA).
- Better coordination must be planned in the future together with other observers, teams or active programs, and also upon checking the CALL website.[18]
- Especially slow rotators and objects with periods matching our diurnal rate should be covered by smaller telescopes (<1 m) which can access many nights, preferably by teaming with observers from other continents.
- Larger facilities which can access only a limited time (few hours, one or few nights) should better target smaller objects (up to few hundred meters) which typically rotate faster and should be able to be solved in the short time available.
- Our LiDAS pipeline has been very efficient and essential for nightly planning, being used day and night during the runs for preliminary reduction of most targets, while Canopus and *Asteroid Light Curve* software were used for final calibration, multi-night linkage and Fourier fitting.
- 18 of our targets do not have yet any published periods and we could solve or constrain periods for 16 of them.
- We *secured periods* for 45 targets (with $P$ given in bold in Table 2) which should be regarded with high confidence $U \sim 3$ (ALCDEF uncertainty code) and which should improve previous results.

---

[18] http://www.minorplanet.info/call.html.

- We found *candidate periods* for 16 targets (given in normal notation in $P$ column in Table 2), corresponding to relative secure fits which either do not match former results, were affected by poor weather, bright Moon (causing larger uncertainties) or have very low amplitude more difficult to solve, all to be regarded with some uncertainty $U \sim 2$.
- We found *tentative periods* for 32 targets (whose $P$ are included in parentheses in Table 2), meaning that no period fitting could be done or was very risky to attempt due to their insufficient coverage or very low amplitude, for which only some lower limit or an approximate period could be stated, all to be regarded with caution and probably $U \sim 1$.
- Finally, 3 objects were observed only few hours (due to bad weather), insufficient to attempt any fit.
- We observed 7 known or candidate binary NEAs and could derive main and secondary periods for 3 targets (2102 Tantalus, 5143 Heracles and 68348) and probably discovered one new binary NEA (2011 WO41).
- We observed 8 known or candidate tumbling NEAs, confirming slow rotation for at least 5 objects and deriving the main periods $P1$ for 3 NEAs (9400, 242708 and 470510).
- We observed rapid oscillations (few minutes) and could derive fast periods $P2$ for 8 larger newly suggested tumbling or binary candidates, including 2 previously supposed tumblers (391033 and 429584), 5 unknown systems (27346, 112985, 285625, 377732, 408980) and one probable binary (2011 WO41) whose periods were solved. Part of another run in Tenerife we could confirm the rapid oscillations of 3 systems (to be presented in our next paper).
- We observed 4 special NEAs, namely 2 space mission targets (163249 and 101955 Bennu), the very fast rotator NEA discovered by EURONEAR (2014 NL52) and the "Halloween Asteroid" (2015 TB145).
- Thanks to the Mercator simultaneous 3 band MAIA imaging, clear variations along the spin rate were evidenced for the first time in color lightcurves of 10 NEAs, and periods derived from the $g - r$ color lightcurves were found to match individual band fits for 4 NEAs (27346, 86067, 112985 and 275976), proving changing morphology or albedo across their surfaces.
- This paper is the second part of a series of four photometry plus one spectroscopy papers which include data of a larger NEA sample to be analised in a future science paper.

## Appendix: Plots of Poorly Observed Objects
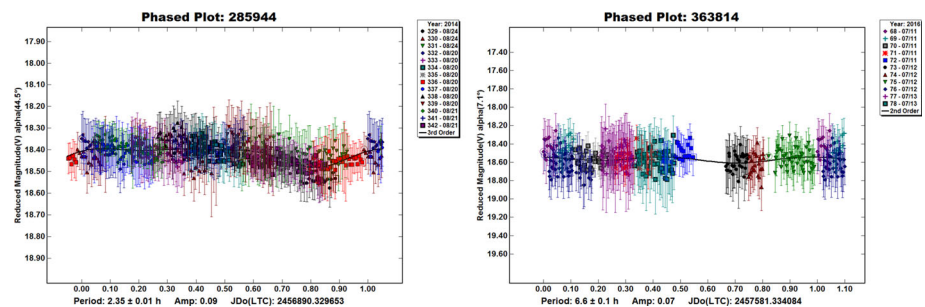
**Fig. 12** Lightcurves of NEAs poorly observed with BUC-T50
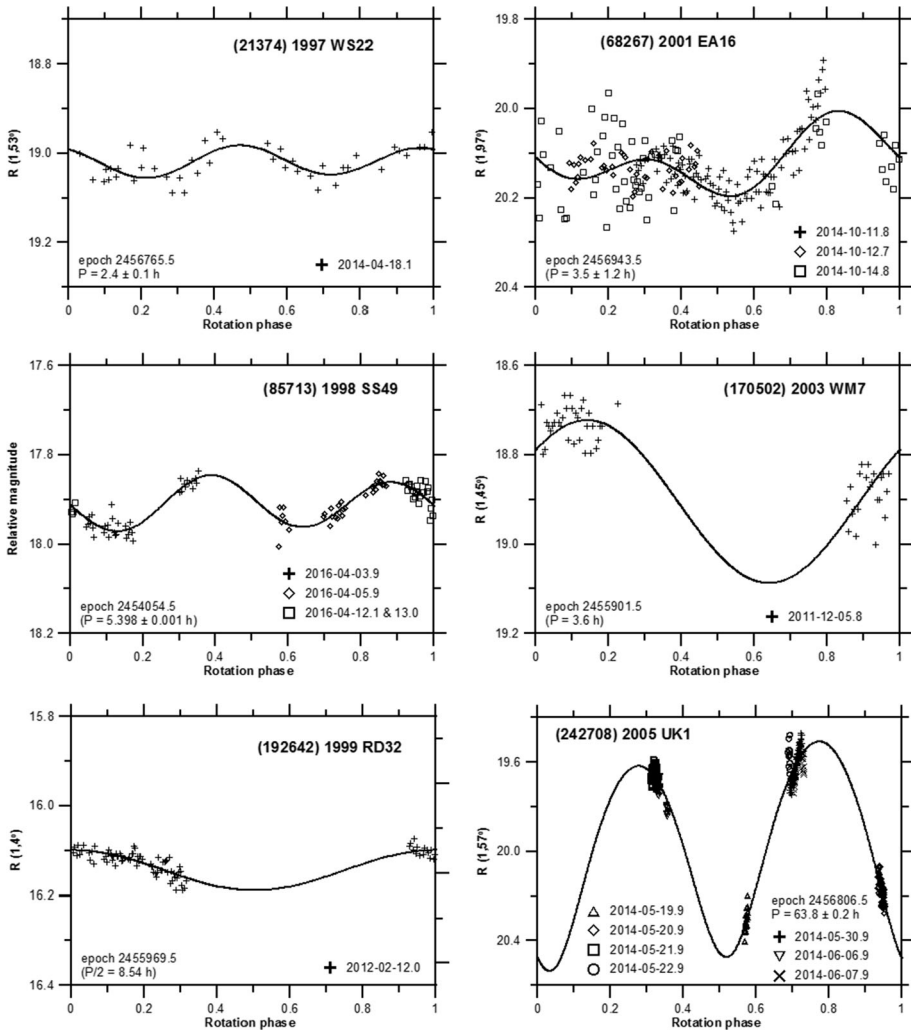
**Fig. 13** Lightcurves of NEAs poorly observed with MOD-T60
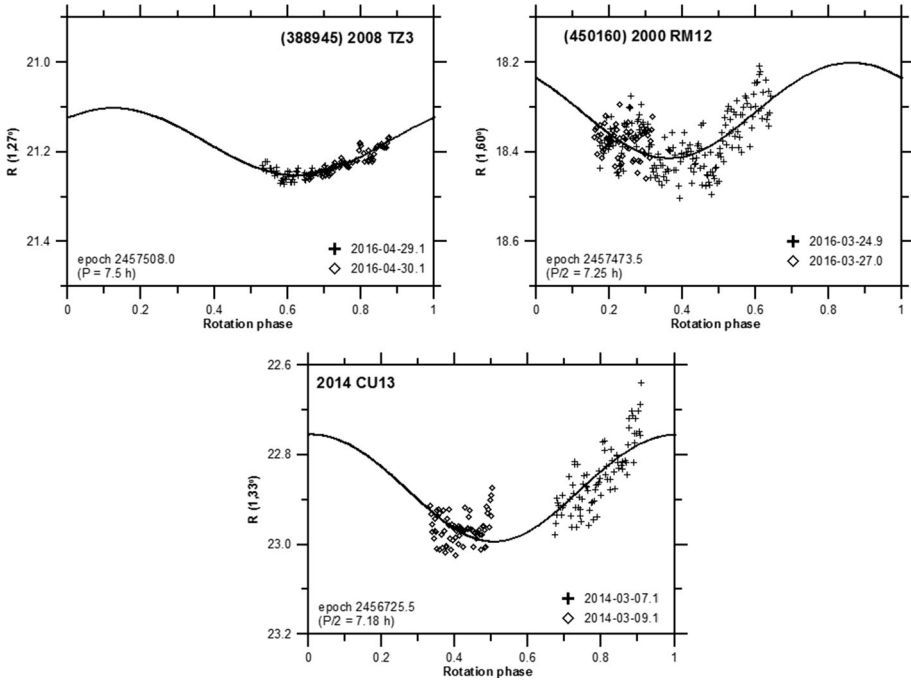
**Fig. 13** continued
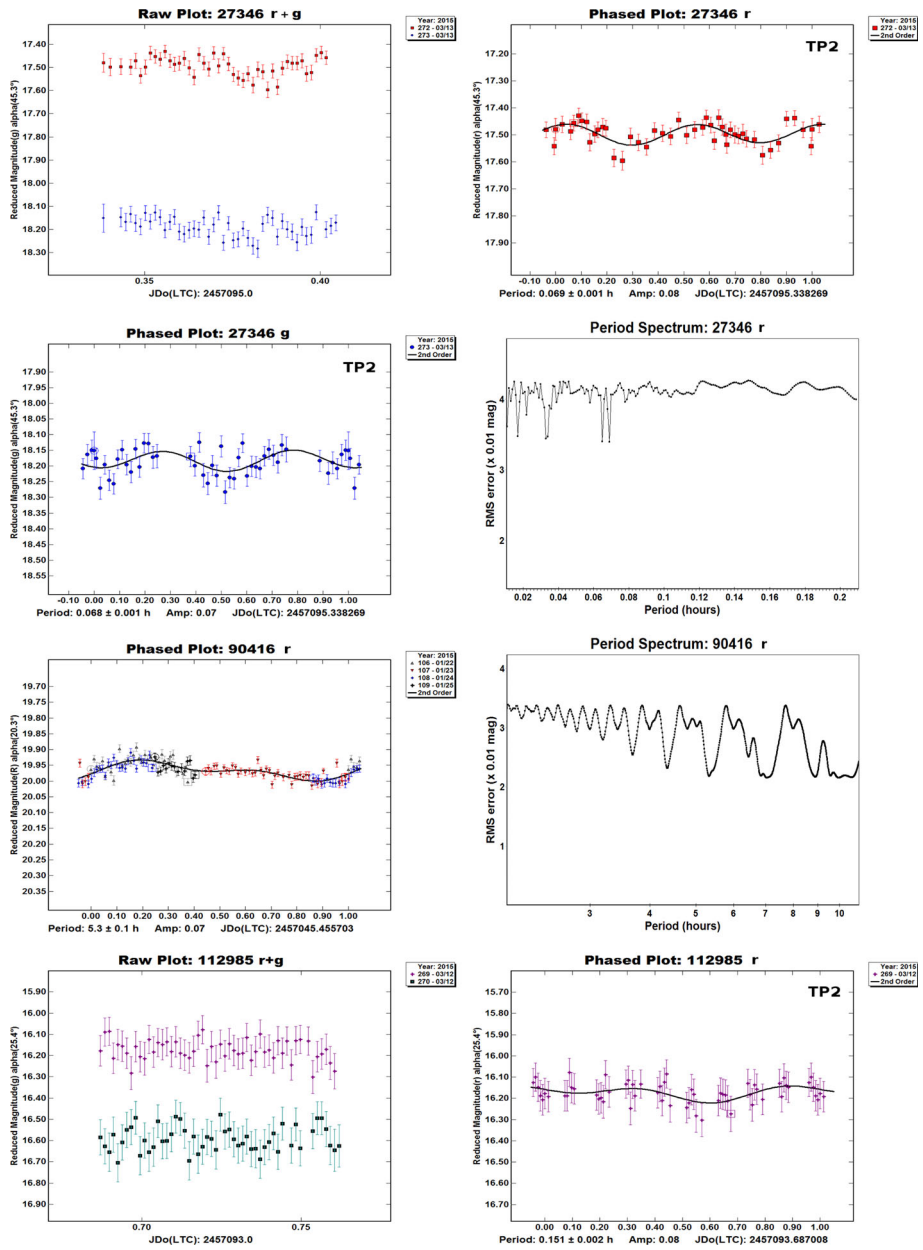
**Fig. 14** Lightcurves of NEAs poorly observed with ORM-Mercator telescope
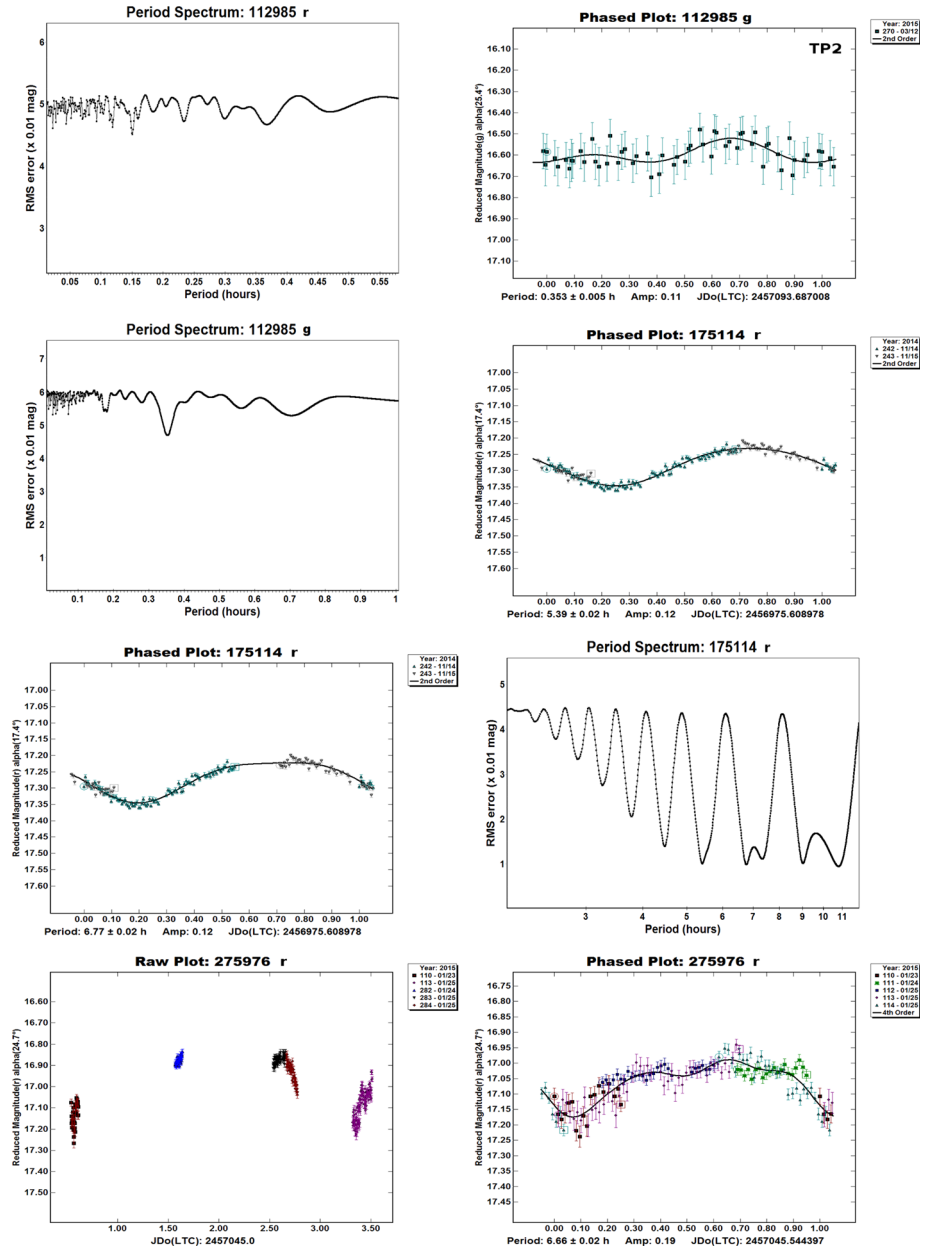
**Fig. 14** continued
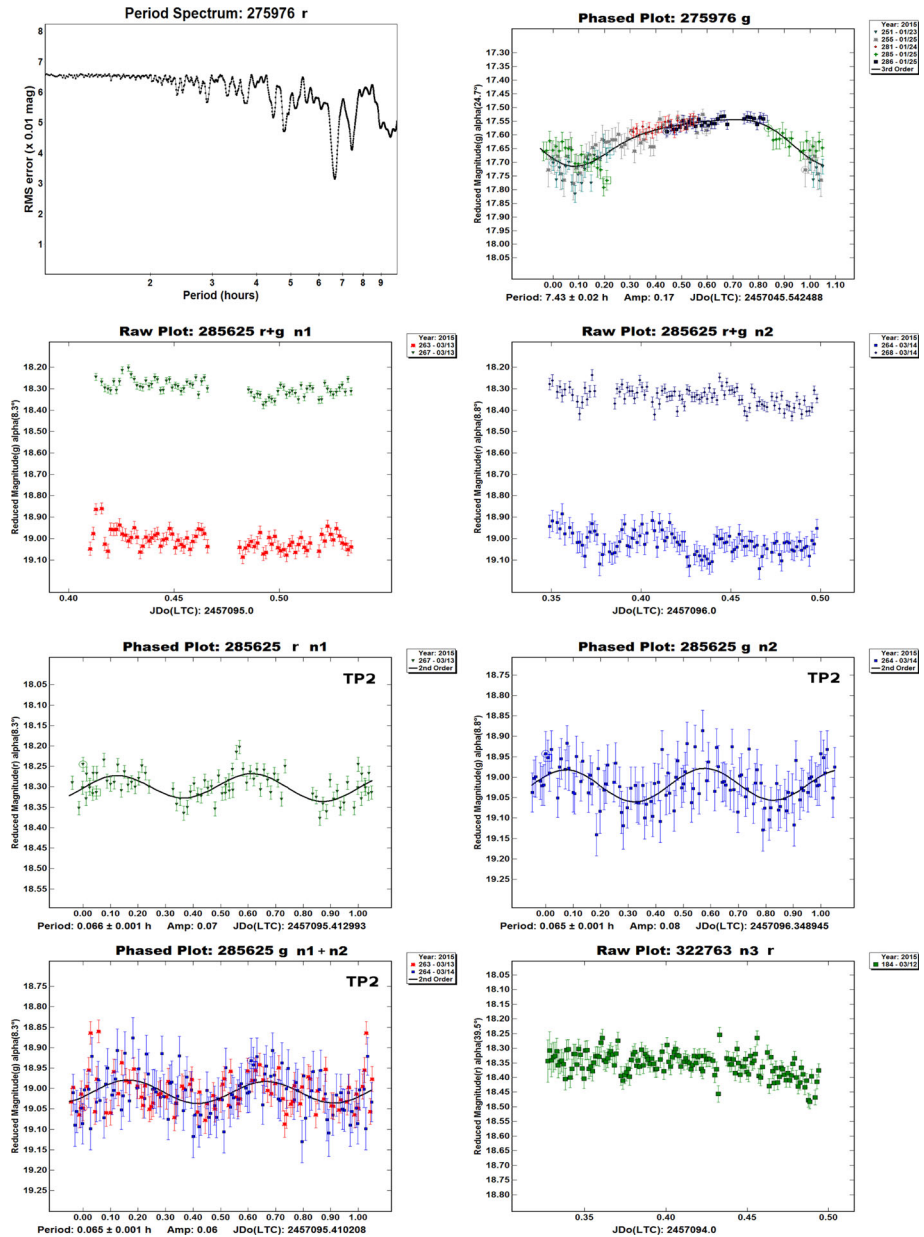
**Fig. 14** continued
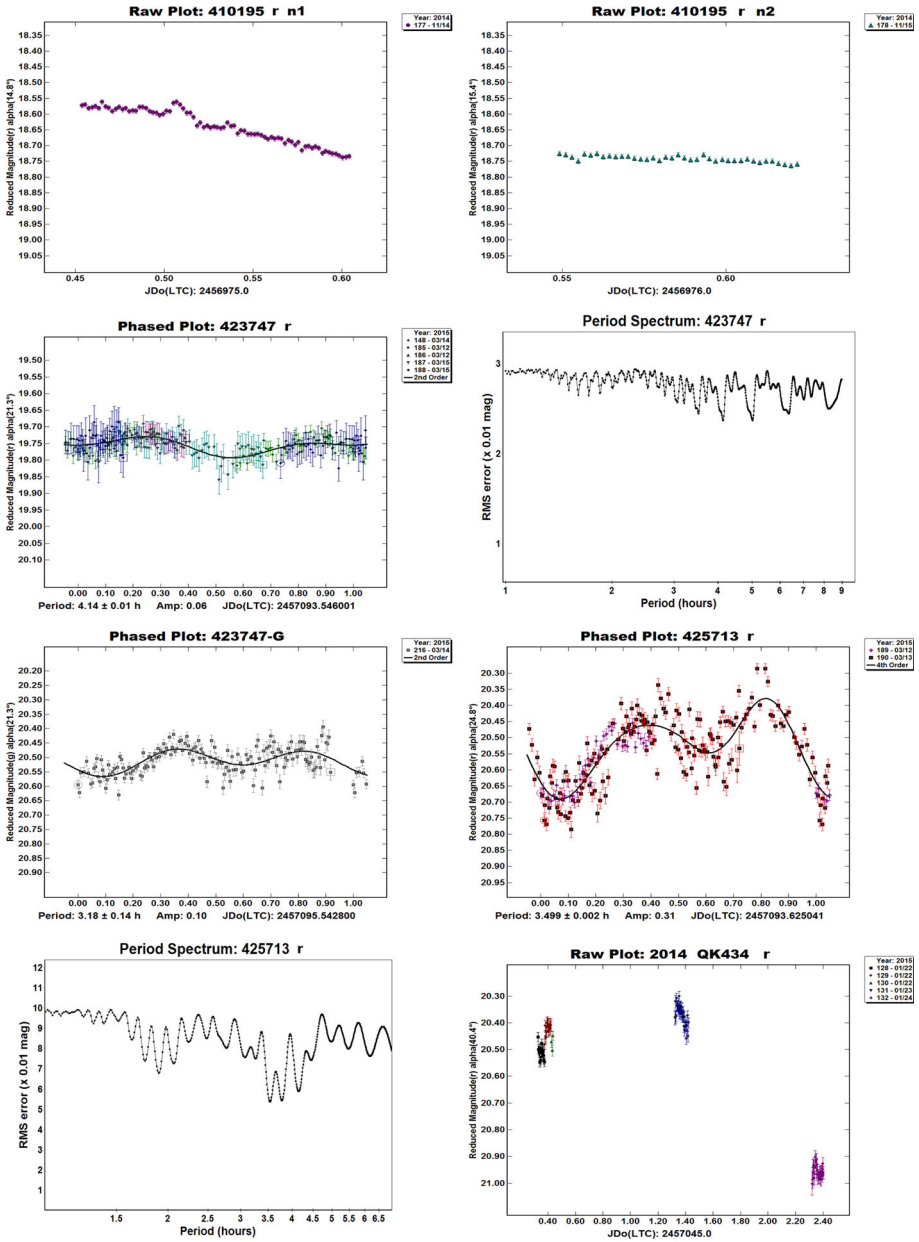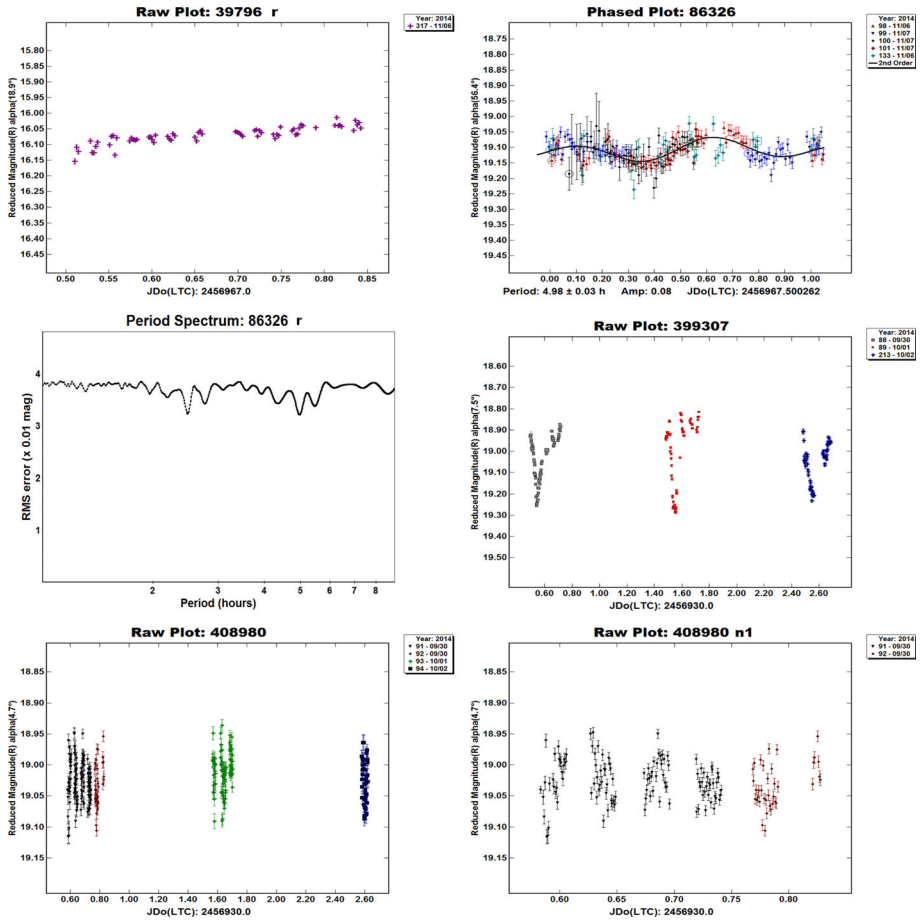
**Fig. 14** continued

Fig. 15 Lightcurves of NEAs poorly observed with LS-Danish telescope
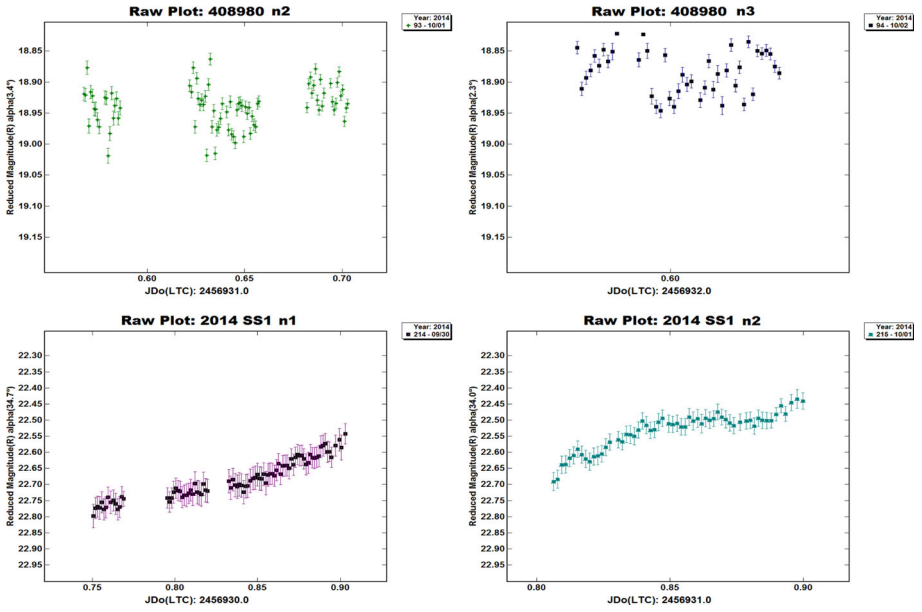
**Fig. 15** continued
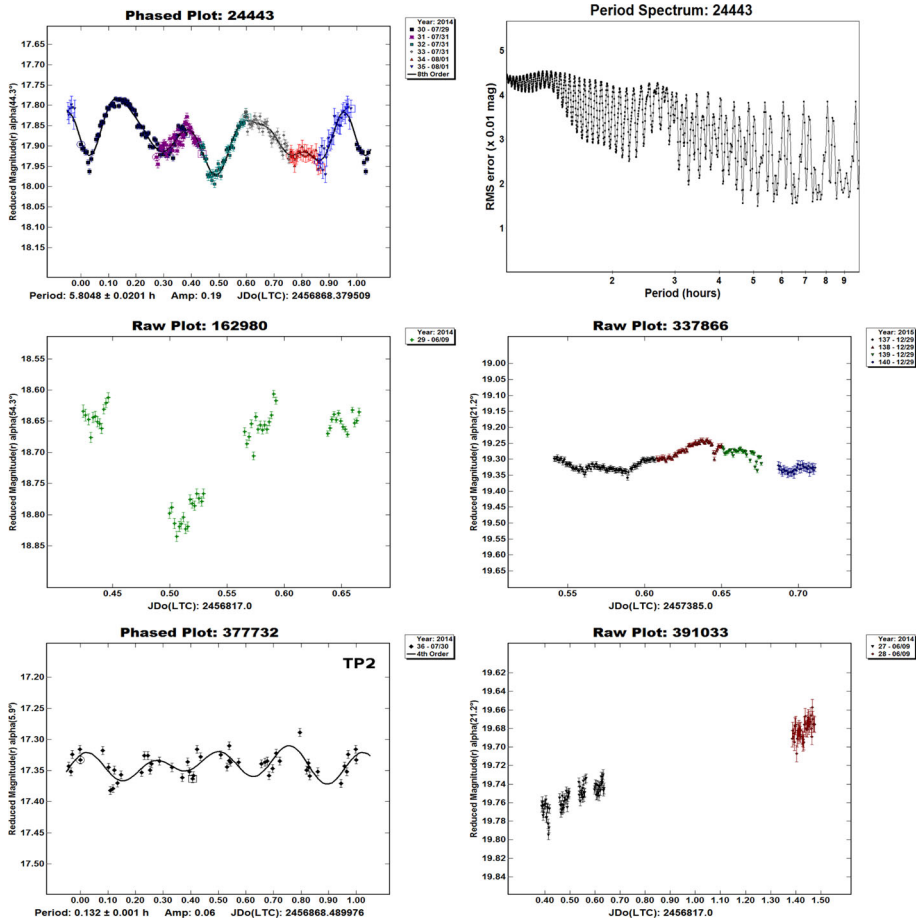
**Fig. 16** Lightcurves of NEAs poorly observed with ORM-INT telescope
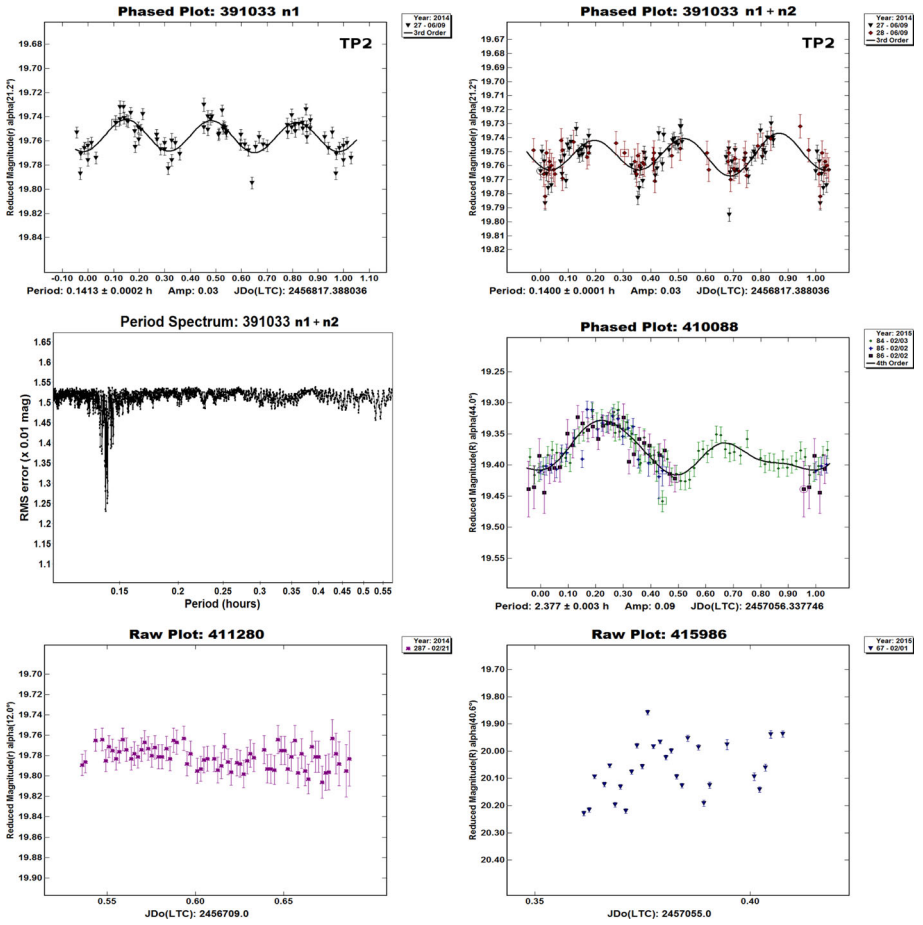
**Fig. 16** continued
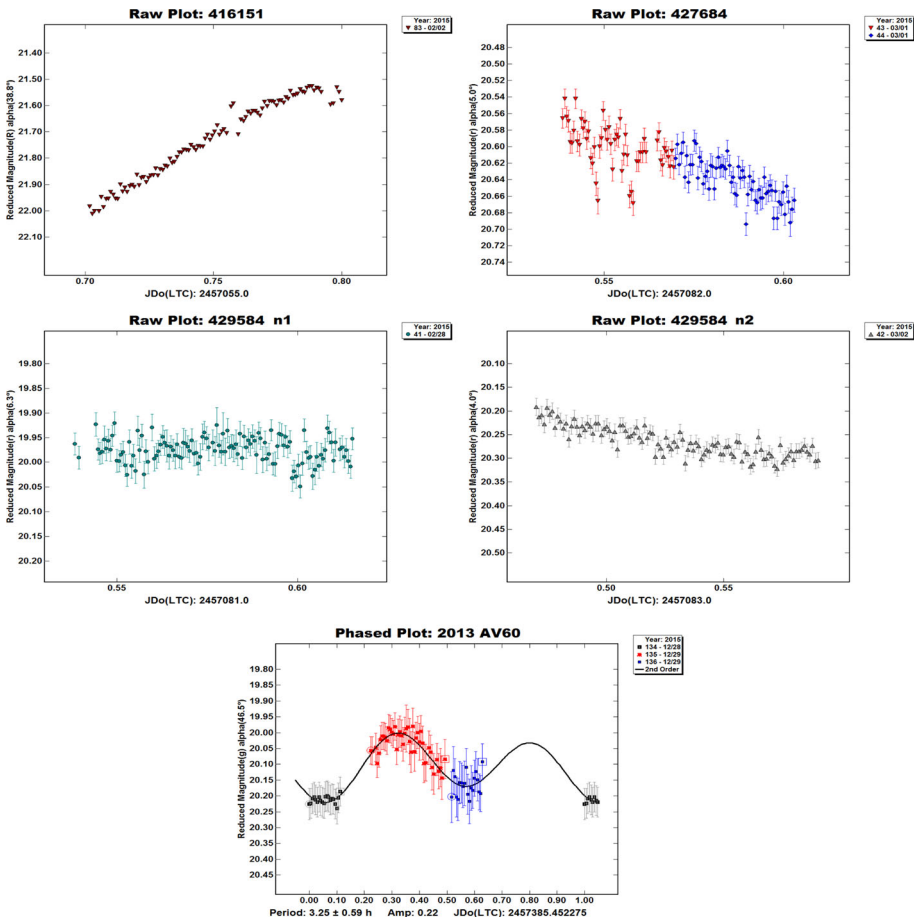
Fig. 16 continued
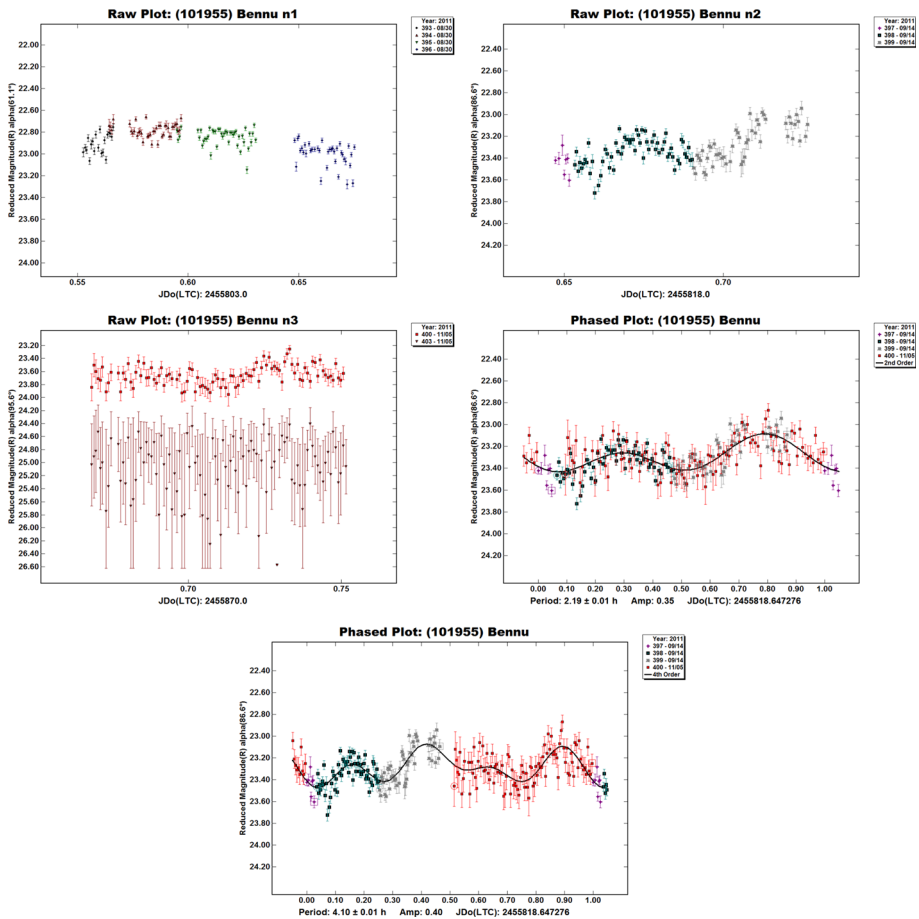
**Fig. 17** Lightcurve of PHA Bennu poorly observed with ORM-WHT telescope

# References

A. Aznar Macias, et. al. EURONEAR—First Lightcurves and Physical Properties of Near Earth Asteroids, accepted, Rom. J. Phys. http://www.nipne.ro/rjp/accepted_papers.html (2017)

A. Aznar Macias, Propiedades fisicas del NEA binario 5143 Heracles (in Spanish), to be published in AstronomíA Magazine **215**, 44 (2017)

L. Benner et al., Radar observations of asteroid 1999 JM8. Meteor. Planet. Sci. **37**(6), 779 (2002)

W.F. Bottke Jr., H.J. Melosh, Binary asteroids and the formation of doublet craters. Icarus **124**, 372 (1996)

E. Bowell et al., A possible satellite of Herculina. Bull. Am. Astron. Soc. **10**, 594 (1978)

A. Carbognani, Asteroids lightcurves at OAVDA: 2013 Dec–2014 Jun (21374, 242708). Minor Planet Bull. **41**, 265 (2014)

A. Carbognani, L. Buzzi, Asteroids lightcurves analysis: 2015 Oct–Dec (337866). Minor Planet Bull. **43**, 162 (2016)

A. Cellino et al., Genetic inversion of sparse disk-integrated photometric data of asteroids: application to Hipparcos data. Astron. Astrophys. **506**, 935 (2009)

A. Cellino et al., Do we observe light curves of binary asteroids? Astron. Astrophys. **144**, 355 (1985)

R. Cornea, O. Vaduvescu, M. Predatu. EURONEAR NEA Lightcurve Survey Tenerife 2015, in work (2017)

R. Dymock, R. Miles, A method for determining the V magnitude of asteroids from CCD images. J. Br. Astron. Assoc. **119**(3), 149 (2009)

L. Elenin et al., Low amplitude lightcurve for km-sized NEA (285944) 2001 RZ11. Minor Planet Bull. **42**, 34 (2015)

A. Galád et al., Joint lightcurve observations of 10 near-earth Asteroids from Modra and Ondřejov. Earth Moon Planet. **97**, 147 (2005)

A.W. Harris et al., Photoelectric observations of asteroids 3, 24, 60, 261, and 863. Icarus **77**(1), 171 (1989)

A.W. Harris, Tumbling Asteroids. Icarus **107**, 209 (1994)

C.W. Hergenrother et al., *Lightcurve and Phase Function Photometry of the OSIRIS-REx Target (101955) 1999 RQ36, 43rd Lunar and Planetary Science Conference* (Texas, USA, 2012)

C.W. Hergenrother et al., Lightcurve, color and phase function photometry of the OSIRIS-REx target asteroid (101955) Bennu. Icarus **226**, 663 (2013)

J.A. Howell, Lightcurve analysis of NEA 3352 McAuliffe. Minor Planet Bull. **39**, 157 (2012)

R.S. Hudson, S.J. Ostro, Shape and non-principal axis spin state of asteroid 4179 Toutatis. Science **270**(5233), 84 (1995)

M. Kaasalainen, Interpretation of lightcurves of precessing asteroids. Astron. Astrophys. **376**, 302 (2001)

D. Kinoshita et al., Surface heterogeneity of 2005 UD from photometric observations. Astron. Astrophys. **466**, 1153 (2007)

B. Koehn et al., Lowel observatory NEA photometric survey (NEAPS)—Jan–Jun 2009 (2009 DO111). Minor Planet Bull. **41**, 295 (2009)

Y.N. Krugly et al., The near-earth objects follow-up program. IV. CCD Photometry in 1996–1999. Icarus **158**(2), 294 (2002)

T. Kwiatkowski et al., Photometric survey of the very small near-earth asteroids with the SALT telescope. I. Lightcurves and periods for 14 objects. Astron. Astrophy. **509**, 94 (2005)

T. Kwiatkowski, Photometric survey of the very small near-earth asteroids with the SALT telescope. II. Discussion of YORP. Astron. Astrophys. **509**, 95 (2005)

T. Kwiatkowski et al., Photometric survey of the very small near-Earth asteroids with the SALT telescope. III. Lightcurves and periods for 12 objects and negative detections. Astron. Astrophys. **511**, 49 (2005)

J.L. Margot et al., Binary asteroids in the near-earth object population. Science **296**, 1445 (2002)

J. Masiero et al., The thousand asteroid light curve survey. Icarus **204**, 145 (2009)

W.J. Merline et al., Discovery of a moon orbiting the asteroid 45 Eugenia. Nature **401**, 565 (1999)

W.J. Merline, et al. Asteroids Do Have Satellites. in Asteroids III, p. 289, 785 pages, (Univ of Arizona Press, 2002)

S. Mottola et al., The slow rotation of 253 Mathilde. Space Sci. **43**, 1609 (1995)

T.G. Muller et al., Large Halloween asteroid at lunar distance. Astron. Astrophys. **598**, 63 (2017)

M.C. Nolan et al., Shape model and surface properties of the OSIRIS-REx target Asteroid (101955) Bennu from radar and lightcurve observations. Icarus **226**, 629 (2013)

F. Ochsenbein et al., The VizieR database of astronomical catalogues. Astron. Astrophys. **143**, 23 (2000)

J. Oey, R. Groom, Photometric observations of near-earth asteroid (348400) 2005 JF21. Minor Planet Bull. **43**, 208 (2016)

B.D. Pilcher, Rotation period determination of 5143 Heracles. Minor Planet Bull. **39**, 148 (2012)

D. Polishook et al., Asteroid rotation periods from the Palomar Transient Factory survey. Mon. Not. R. Astron. Soc. **421**, 2094 (2012)

M. Popescu et al., Spectral properties of eight near-earth asteroids. Astron. Astrophys. **535**, 15 (2011)

M. Popescu et al., Spectral properties of the largest asteroids associated with Taurid Complex. Astron. Astrophys. **572**, 106 (2014)

M. Popescu, et. al., *Visible spectra of near-Earth asteroids obtained with the Isaac Newton Telescope*, to be submitted soon (2017)

P. Pravec et al., CCD photometry of 6 near-earth asteroids. Earth Moon Planet. **71**, 177 (1995)

P. Pravec et al., Lightcurves of 7 near-earth asteroids. Icarus **124**, 471 (1996)

P. Pravec et al., The near-earth objects follow-up program II. Results for 8 asteroids from 1982 to 1995. Icarus **130**, 275 (1997)

P. Pravec, G. Hahn, Two-period lightcurve of 1994 AW1: indication of a binary asteroid? Icarus **127**, 431 (1997)

P. Pravec et al., Lightcurves of 26 near-earth asteroids. Icarus **136**, 124 (1998)

P. Pravec et al., Occultation/eclipse events in binary asteroid 1991 VH. Icarus **133**, 79 (1998)

P. Pravec et al., Two periods of 1999 HF1—another binary NEA candidate. Icarus **158**, 276 (2002)

P. Pravec et al., Tumbling asteroids. Icarus **173**, 108 (2005)

P. Pravec et al., Photometric survey of binary near-earth asteroids. Icarus **181**, 63 (2006)

P. Pravec, et. al., NEA rotations and binaries, in Near Earth Objects, our Celestial Neighbors: Opportunity and Risk, Proceedings of IAU Symposium 236. (Cambridge University Press, Cambridge, 2007) p. 167

P. Pravec, A.W. Harris, Binary asteroid population. 1. Angular momentum content. Icarus **190**, 250 (2007)

P. Pravec et al., Binary asteroid population. 2. Anisotropic distribution of orbit poles of small, inner main-belt binaries. Icarus **218**, 125 (2012)

P. Pravec et al., The tumbling spin state of (99942) Apophis. Icarus **233**, 48 (2014)

P. Pravec et al., Binary asteroid population. 3. Secondary rotations and elongations. Icarus **267**, 267 (2016)

E.G. Rivera-Valentin et al., (163693) ATIRA (binary detection). CBET **4347**, 1 (2017)

T. Sekiguchi et al., Bicolour lightcurve of TNO 1996 TO66 with the ESO-VLT. Astron. Astrophys. **385**, 281 (2002)

B. Skiff, Posting on CALL web site. http://www.minorplanet.info/call.html (2011)

B. Skiff et al., Lowell observatory near-earth asteroid photometric survey (NEAPS)—2008 May through 2008 December. Minor Planet Bull. **39**, 111 (2012)

J.R. Spencer et al., The lightcurve of 4179 Toutatis: evidence for complex rotation. Icarus **117**, 71 (1995)

R.F. Stellingwerf, Period determination using phase dispersion minimization. Astrophys. J. Part 1 **224**, 953 (1978)

A. Thirouin et al., The mission accessible near-earth objects survey (MANOS): first photometric results. Astron. J. **152**, 163 (2016)

O. Vaduvescu, First EURONEAR NEA discoveries from La Palma using the INT. Mon. Notices R. Astron. Soc. **449**, 1614 (2015)

B.D. Warner, *A Practical Guide to Lightcurve Photometry and Analysis*, 2nd edn. (Springer, New York, 2006)

B.D. Warner, The asteroid lightcurve database. Icarus **202**, 134 (2009)

B.D. Warner, Asteroid lightcurve analysis at palmer divide observatory: 2011 Dec–2012 Mar (3352 McAuliffe). Minor Planet Bull. **39**, 158 (2012)

B.D. Warner, R. Megna, Lightcurve analysis of NEA (192642) 1999 RD32. Minor Planet Bull. **39**, 154 (2012)

B.D. Warner, NEA lightcurve analysis at CS3-PDS: 2014 Jan–Mar (68031). Minor Planet Bull. **41**, 159 (2014)

B.D. Warner, NEA lightcurve analysis at CS3-PDS: 2014 Mar–Jun (21374). Minor Planet Bull. **41**, 214 (2014)

B.D. Warner, NEA lightcurve analysis at CS3-PDS: 2014 Mar–Jun (2014 CU13). Minor Planet Bull. **41**, 160 (2014)

B.D. Warner, NEA lightcurve analysis at CS3-PDS: 2013 Sep–Dec (411280 = 2010 SL13). Minor Planet Bull. **41**, 115 (2014)

B.D. Warner, NEA lightcurve analysis at CS3-PDS: 2013 Jun–Sep (9950 ESA). Minor Planet Bull. **41**, 41 (2014)

B.D. Warner, NEA lightcurve analysis at CS3-PDS: 2015 Jan–Mar (410088, 416151 and 427684). Minor Planet Bull. **42**, 177 (2015)

B.D. Warner, NEA lightcurve analysis at CS3-PDS: 2015 Jan–Mar (159533). Minor Planet Bull. **42**, 119 (2015)

B.D. Warner, NEA lightcurve analysis at CS3-PDS: 2015 Jan–Mar (90416). Minor Planet Bull. **42**, 175 (2015)

B.D. Warner, NEA lightcurve analysis at CS3-PDS: 2015 Jan–Mar (2014 QK434). Minor Planet Bull. **42**, 178 (2015)

B.D. Warner, NEA lightcurve analysis at CS3-PDS: 2015 Jan–Mar (39796). Minor Planet Bull. **42**, 174 (2015)

B.D. Warner, NEA lightcurve analysis at CS3-PDS: 2014 Jun–Oct (86326). Minor Planet Bull. **42**, 115 (2015)

B.D. Warner, (399307) 1991 RJ2: a new NEA binary discovery. Minor Planet Bull. **42**, 37 (2015)

B.D. Warner, NEA lightcurve analysis at CS3-PDS: 2014 Jun–Oct (408980 = 2002 RB126). Minor Planet Bull. **42**, 49 (2015)

B.D. Warner, NEA lightcurve analysis at CS3-PDS: 2014 Jun–Oct (2014 SS1). Minor Planet Bull. **42**, 50 (2015)

B.D. Warner, NEA lightcurve analysis at CS3-PDS: 2014 Jun–Oct (162980). Minor Planet Bull. **42**, 46 (2015)

B.D. Warner, A quartet of NEA binary candidates (2102 Tantalus and 68348). Minor Planet Bull. **42**, 79 (2015)

B.D. Warner, NEA lightcurve analysis at CS3-PDS: 2014 Jun–Oct (391033). Minor Planet Bull. **42**, 47 (2015)

B.D. Warner, NEA lightcurve analysis at CS3-PDS: 2014 Jun–Oct (112985). Minor Planet Bull. **42**, 259 (2015)

B.D. Warner, NEA lightcurve analysis at CS3-PDS: 2014 Jun–Oct (86067). Minor Planet Bull. **42**, 172 (2015)

B.D. Warner, NEA lightcurve analysis at CS3-PDS: 2014 Jun–Oct (85713). Minor Planet Bull. **42**, 43 (2015)

B.D. Warner, NEA lightcurve analysis at CS3-PDS: 2014 Jun–Oct (429584). Minor Planet Bull. **42**, 172 (2015)

B.D. Warner, NEA lightcurve analysis at CS3-PDS: 2016 Apr–Jul (141354). Minor Planet Bull. **43**, 315 (2016)

B.D. Warner, NEA lightcurve analysis at CS3-PDS: 2016 Jan–Apr (450160 = 2000 RM12). Minor Planet Bull. **43**, 245 (2016)

B.D. Warner, NEA lightcurve analysis at CS3-PDS: 2016 Jan–Apr (337866). Minor Planet Bull. **43**, 244 (2016)

B.D. Warner, NEA lightcurve analysis at CS3-PDS: 2016 Apr–Jul (9400). Minor Planet Bull. **43**, 312 (2016)

B.D. Warner, NEA lightcurve analysis at CS3-PDS: 2015 Jun–Sep (9400, 112985). Minor Planet Bull. **43**, 67 (2016)

B.D. Warner, NEA lightcurve analysis at CS3-PDS: 2015 Oct–Dec (112985). Minor Planet Bull. **43**, 146 (2016)

B.D. Warner, NEA lightcurve analysis at CS3-PDS: 2016 Apr–Jul (388945). Minor Planet Bull. **43**, 311 (2016)

B.D. Warner, NEA lightcurve analysis at CS3-PDS: 2016 Oct–Dec (3352). Minor Planet Bull. **44**, 98 (2017)

B.D. Warner, NEA lightcurve analysis at CS3-PDS: 2016 Jul–Sep (3352 McAuliffe). Minor Planet Bull. **44**, 23 (2017)

B.D. Warner, NEA lightcurve analysis at CS3-PDS: 2016 Jul–Sep (470510). Minor Planet Bull. **44**, 30 (2017)

B.D. Warner, A. Aznar, A. Sotta, Lightcurve analysis of the NEA 2016 NL15. Minor Planet Bull. **44**(2), 157 (2017)

A. Waszczak et al., Asteroid light curves from the Palomar Transient Factory survey: rotation periods and phase functions from sparse photometry. Astron. J. **150**, 75 (2015)

F. Yoshida et al., Photometric observations of a very young family-member asteroid (832) Karin. Publ. Astron. Soc. Jpn. **56**, 1105 (2004)